Roles of LewisC-containing N-glycan whose expression is developmentally regulated on cell-cell interaction in the mouse brain

Handa-Narumi, Mai

DOCTOR OF PHILOSOPHY

Department of Physiological Sciences
School of Life Science
SOKENDAI (The Graduate University for Advanced Studies)

2016

Acknowledgements

First of all, I would like to show my heartfelt gratitude to my advisor Prof. Kazuhiro Ikenaka of National Institute for Physiological Sciences for offering me a wonderful opportunity to study in his laboratory. I appreciate his constant support and communication during my research with his patience, enthusiasm, and stupendous knowledge, which guided me through research and writing this thesis.

I express my deepest appreciation to Dr. Takeshi Yoshimura for his valuable instructions and complaisant teaching during my research.

I also express special thanks to Dr. Seiji Hitoshi, Dr. Kenji Tanaka, Dr. Nobuhiko Ohno, and Dr. Takeshi Shimizu for providing me numerous ideas, relevant discussions and help during my work.

I thank Prof. Hiroshi Kiyama and Dr. Hiroyuki Konishi of Division of Functional Anatomy and Neuroscience, Nagoya University Graduate School of Medicine for investigation of siglec-H-sugar chain cluster interaction by Biacore and stimulating discussions.

I thank Prof. Koichi Fukase and Dr. Yoshiyuki Manabe of Department of Chemistry, Graduate School of Science Osaka University for kindly providing sugar chain clusters to me and for useful discussions.

I thank Dr. Tosifusa Toda (Proteome Research Center, Department of Research Support and coordination, Advanced Medical Research Center, Yokohama City University) for helpful advice on 2D-PAGE; Dr. Yuko Fukata and Dr. Atsushi

Sekiya (Division of Membrane Physiology, National Institute for Physiological Sciences) for valuable advice and discussions on immunocytochemistry and biochemical experiments; Ms. Yuko Mori and Ms. Yumiko Makino of Functional Genomics Facility, NIBB Core Research Facilities for analyzing my samples by LC-MS and providing faithful data to me.

I also thank the member of sugar chain group: Mr. Yuichiro Kano, Ms. Isoko Ito, and Ms.Takako Koike. They technically supported my experiments of sugar chains. Especially, Ms. Ito and Ms. Koike taught me many useful methods for sugar chain analysis when I came in this laboratory.

Beside my supervisors, I would like to thank members of my thesis committee; Prof. Motohiro Nishida, Prof. Masaki Fukata, and Prof. Ken Kitajima for their encouragement, insightful comments, and questions.

I thank my fellow lab members in Prof Ikenaka' s lab: Dr. Naoko Inamura, Dr. Yugo Ishino, Dr. Noriyoshi Usui, Dr. Takahiro Shimizu, Dr. Shota Sugio, Dr. Hirokazu Hashimoto, Dr. Wilaiwan Wisessmith, Dr. Yasuyuki Osanai, Dr. Jiang Wen, Dr. Kazuo Kunisawa, Li Jia Yi, Saori Kikuchihara, and Ms. Rie Taguchi for discussions, supports, and for all the fun we had in the last five years.

Finally, I want to appreciate my father, mother, sister, and brother. I also want to appreciate my husband. They understood my feeling, condition and supported me for a long time. Thank them for everything they have done for me.

This work was supported by Grant-in-Aid for JSPS Fellows Number 26・3075.

Table of Contents

Abbreviations

Asn: asparagine residue

BPB: bromophenol blue

CBB: Coomassie Brilliant Blue

CDG: congenital disorders of glycosylation

CHAPS: 3-((3-cholamidopropyl) dimethylammonium)-1-propanesulfonate

CRT: calreticulin

DEAE: diethylaminoethyl

DTT: dithiothreitol

ER: endoplasmic reticulum

Fuc: fucose

Gal: galactose

GalNAc: N-acetylgalactosamine

GlcNAc: N-acetylglucosamine

HPLC: high performance liquid chromatography

IEF: isoelectric focusing

ITAM: immunoreceptor tyrosine-based activation motif

ITIM: immunoreceptor tyrosine-based inhibition motif

LAMP: limbic system-associated membrane protein

LC-MS: Liquid chromatography-mass spectrometry

LeC: LewisC

MAG: myelin-associated glycoprotein

Man: mannose

MW: molecular weight

NEM: N-ethylmaleimide

NeuAc: N-acetylneuraminic acid

NP: normal phase

NTM: neurotrimin

PMSF: phenylmethylsulfonyl fluoride

PVDF: polyvinylidene difuloride

PBS: phosphate-buffered saline

PFA: paraformaldehyde

RP: reverse phase

SB-10: sulfobetaine-10

Ser: serine residue

SDS-PAGE: sodium dodecyl sulfate-polyacrylamide gel electrophoresis

Siglec: sialic acid binding Ig-like lectin

SPR: surface plasmon resonance

TFA: trifluoroacetic acid

TfR: transferrin receptor

Thr: threonine residue

WB: Western blot analysis

2D-PAGE: two-dimensional polyacrylamide gel electrophoresis

2-AP: 2-aminopyridine

6SLeC: 6-sialyl-LewisC

Summary

Glycosylation of proteins is one of the major posttranslational modifications. N-glycans harbored on membrane proteins profoundly affect the character of proteins by altering their structure or capacity to bind to other molecules. Various types of N-glycans are synthesized in the endoplasmic reticulum and Golgi apparatus. Proper N-glycosylation of proteins is important for normal brain development and multiple functions of nervous system.

Sialic acid is an acidic monosaccharide present at the non-reducing terminal of sugar residues attached through α2,3-, α2,6- or α2,8-linkage. Sialylated A2G'2F (Figure 1A) is one of the major N-glycans, most of which contains "6-sialyl-LewisC (6SLeC)" [Galβ(1-3){NeuAcα(2-6)}GlcNAc-] moiety. The level of sialylated A2G'2F increased during development. These observations suggest that 6SLeC-containing sialylated A2G'2F plays a role in the development and/or maintenance of the mouse brain.

I analyzed sialylated N-glycans contained in 12-week-old mouse brain by high performance liquid chromatography (HPLC), and I detected non-, mono-, di-, tri, tetra-sialylated A2G'2F in addition to our previous report. Biosynthetic pathway of 6SLeC-containing sialylated A2G'2F was deduced from these results. I also analyzed N-glycans contained in subcellular fractionated proteins from 12-week-old mouse brain. Sialylated A2G'2F accumulated in membrane and synaptosomal fraction. These data suggest sialylated A2G'2F mainly localized on plasma membrane and synaptosome.

Sialic acid binding Ig-like lectins (Siglec) distinguish linkage types of sialic acids. Some of the siglecs are crucial for exerting brain function. I predicted that 6SLeC plays a role in adult mouse brain through 6SLeC-siglec interactions. To demonstrate this hypothesis, determination of sialylated A2G'2F-carrier proteins and 6SLeC-recognizing proteins are required.

First I tried to identify sialylated A2G'2F-carrier proteins. We previously improved the method for analyzing N-glycan on glycoproteins in the sodium dodecyl sulfate-polyacrylamide gel electrophoresis gel. I homogenized 12-week-old mouse brain and subjected them on a SDS-PAGE. The gel was cut into 20 pieces and N-glycans contained in each gel pieces were analyzed by high performance liquid chromatography. Sialylated A2G'F was detected in particular gel pieces with molecular mass of 50-70 kDa. Synaptosomal fraction was subjected on a two-dimensional polyacrylamide gel electrophoresis and of gel containing 50-70 kDa proteins were cut into 10 pieces. I revealed that restricted number of acidic proteins with molecular mass of 50-70 kDa mainly carry A2G'2F in the synaptosomal fraction. Furthermore, I revealed that A2G'2F was mainly accumulated in Triton X-100-soluble component but not in postsynaptic density of the synaptosomal fraction. I also analyzed proteins in the same gels by liquid chromatography-mass spectrometry, and neurotrimin (NTM) and calreticulin (CRT) were detected. It has been reported that there is a N-glycan whose structure is consistent with A2G'2F on NTM. Thus NTM is a strong candidate for the A2G'2F-carrier. Another candidate was CRT, which is expressed on endoplasmic reticulum and cell surface, but localization in mouse brain was not reported. I performed

Western blot analysis of subcellular fractionated proteins and showed that CRT is not only expressed in ER but also in triton-soluble component of synaptosomal fraction. I observed that CRT was strongly expressed in cultured cortical neurons and CRT signals were apposed to PSD95 signals in some of mature spines. This is the first report that CRT locates in synapses.

Next, I also tried to identify 6SLeC-recognizing siglec. Since ligand glycan for siglec-H is unknown, I chose this siglec for my study. I used Biacore assay to investigate 6SLeC-Siglec-H interaction and applied sugar chain cluster technology to increase the binding affinity of sugar chains against receptor proteins by forming sugar chain cluster on polylysine residue. This approach was successful and I found that 6SLeC interacted with siglec-H. Siglec-H is expressed in microglia and is reported to activate microglial phagocytosis toward glioma cells.

In summary, I found 6SLeC-containing sialylated A2G'2F is harbored on proteins present in the Triton X-100-soluble component of the synaptosomal fraction and can be recognized by microglia expressing siglec-H. This interaction may contribute to the functions of microglia, such as clearance of apoptotic neuron, synapse pruning, and neuroprotection in the mouse brain.

Introduction

Glycosylation of proteins is one of the major posttranslational modifications. N-glycosylation is one type of glycosylation and glycosylates asparagine residues of the protein with Asn-X-Ser/Thr sequence. N-glycans harbored on membrane proteins (glycoproteins) profoundly affect the character of proteins by altering their structure or capacity to bind to other molecules. N-glycan transfer to a protein occurs in the endoplasmic reticulum (ER), followed by processing in the Golgi apparatus [Atkinson and Lee, 1984]. The ER and Golgi apparatus contain many glycosyltransferases and synthesize various N-glycans. Congenital disorders of glycosylation (CDG) result from inborn errors of glycoprotein biosynthesis in human. In most type of CDG, N-glycosylation of various proteins is deficient or defective, resulting in the absence or structural alteration of N-glycans. Abnormalities in the normal brain development and multiple functions of the nervous system are noteworthy phenotype of CDG [Cylwik et al., 2013; Freeze et al., 2005; Varki et al., 2009;]. These observations suggest an importance of N-glycans in the nervous system.

Sialic acid is an acidic monosaccharide present at the non-reducing terminal of sugar residues attached through α2,3-, α2,6- or α2,8-linkage. We previously reported identification of various structures of sialylated and non-sialylated N-glycans in the mouse cerebral cortex [Ishii et al., 2007; Torii, Yoshimura, Narumi et al., 2014]. Among the identified N-glycans, sialylated A2G'2F (Figure 1A) is one of the major N-glycans which contains type 1 antennary [Galβ(1-3)GlcNAc-]. There are two types of

α2,6-sialylated N-glycans. One attaches to the galactose residue at the non-reducing end [NeuAcα(2-6)Gal-] and the other to the GlcNAc residue in the type 1 antennary of N-glycans [Galβ(1-3){NeuAcα(2-6)}GlcNAc-]. We termed the latter structure [Galβ(1-3){NeuAcα(2-6)}GlcNAc-] "6-sialyl-LewisC (6SLeC)". The amount of sialylated A2G'2F with 6SLeC were increased during development [Ishii et al., 2007; Torii et al., 2014]. These observations suggest that 6SLeC-containing sialylated A2G'2F plays a role in the development and/or maintenance of the mouse brain.

Sialic acid binding Ig-like lectins (siglec) distinguish linkage types of sialic acids. Some of the siglecs are crucial for exerting brain function. For example, siglec-4 (MAG) is present in the myelin of central nervous system and recognizes α2,3-linked sialic acid [Lai et al., 1987; Vinson et al., 2001]. This interaction mediates neurite outgrowth [Tang et al., 1997].

I hypothesized that 6SLeC plays a role in the adult mouse brain through 6SLeC-recognizing siglec. To demonstrate this hypothesis, determination of sialylated A2G'2F-carrier proteins and 6SLeC-recognizing proteins are required. I used improved method for analyzing N-glycan on the glycoproteins in the sodium dodecyl sulfate-polyacrylamide gel electrophoresis (SDS-PAGE) gel [Yoshimura, Yamada, Narumi et al., 2012]. Using this method, we achieved high N-glycan recovery rate; we detected N-glycans from 0.5 μg of a glycoprotein was subjected on a SDS-PAGE. I applied this method not only to SDS-PAGE gel but also to two-dimensional polyacrylamide gel electrophoresis (2D-PAGE) gel. In this study, I revealed that restricted number of acidic proteins with molecular mass of 50-70 kDa mainly carry

A2G'2F in the Triton X-100-soluble component (T-sol) of the synaptosomal (Syn) fraction of mouse brain.

Siglec-E is expressed in mouse brain microglia and involved in neuroprotection by preventing phagocytosis and the associated oxidative burst [Claude et al., 2013]. Siglec-E prefers α2,8- and α2,3-linked sialic acid but this siglec also binds to 6SLeC [Redelinghuys et al., 2011].

Siglec-H is a microglia specific siglec, and activation of siglec-H counterbalances the inhibition of siglec-E. However, ligand glycan for this siglec is unknown. I used sugar chain cluster technology to increase the binding affinity of sugar chains against receptor proteins by forming sugar chain cluster on polylysine residue. This approach was successful and I found that 6SLeC interacted with siglec-H.

In summary, I found 6SLeC-containing sialylated A2G'2F is harbored on proteins present in the Triton X-100-soluble component of the synaptosomal fraction and can be recognized by microglia expressing siglec-H. This interaction may contribute to the functions of microglia, such as clearance of apoptotic neuron, synapse pruning, and neuroprotection in the mouse brain.

Materials and Methods

Materials and chemicals

Urea, dithiothreitol (DTT), iodoacetoamide, trifluoroacetic acid (TFA), ammonium bicarbonate, and Silver Stain MS Kit were purchased from Wako (Osaka, Japan). NP-40 was from Sigma (St. Louis, MO, USA) and 3-((3-cholamidopropyl) dimethyl ammonium)-1-propanesulfonate (CHAPS) from Dojindo (Kumamoto, Japan). Sulfobetaine-10 (SB-10) was purchased from Amresco LLC (Solon, OH, USA). Trypsin was from Promega Corporation (Madison, WI, USA) and polyvinylidene difuloride (PVDF) membrane (Immobilon-P, 0.45 μm) was from Merk Millipore (Billerica, MA, USA). IPG buffer (pH 3-11), Immobiline DryStrips (pH 3-11, 13 cm long), and a detection kit for enhanced chemiluminescence (ECL plus) were purchased from GE Healthcare UK Ltd. (Buckinghamshire, England). Anhydrous hydrazine was purchased from Tokyo Chemical Industry (Tokyo, Japan), 2-aminopyridine (2-AP) was from Kanto Chemical (Tokyo, Japan), and dimethylamine borane was from Wako (Osaka, Japan). Graphite carbon columns (GL-Pak Carbograph, Cat. No. 5010–23005) were purchased from GL Science (Tokyo, Japan). Microgranular cellulose for packed cellulose columns was from Merck Millipore. Neuraminidase derived from Arthrobacter ureafaciens was purchased from Nacalai Tesque (Kyoto, Japan). α2,3-sialidase, specific for α2,3-linked sialic acid, was from New England BioLabs (Ipswich, MA, USA). Pyridylaminated (PA)-sugar chains used as standards were purchased from Takara Bio (Tokyo, Japan).

Antibodies

Primary antibodies used in this study were as follows; rabbit anti-calreticulin (CRT) IgG (ab92516, Abcam plc, Cambridge, UK), mouse anti-PSD95 IgG (7E3-1B8, Thermo Fisher Scientific Inc., Waltham, MA, USA), mouse anti-GM130 IgG (610822, Becton Dickinson, NJ, USA), and mouse anti-transferrin receptor (TfR) IgG (136800, Thermo Fisher Scientific Inc.). For immunocyto/histochemistry, Alexa 568-conjugated anti-rabbit IgG (Thermo Fisher Scientific Inc.) and Cy5-conjugated anti-mouse IgG (Merck Millipore) were used as secondary antibodies.

Animals

All mice used in this study were kept in the institutional Center for Experimental Animals with free access to food and water. Timed pregnant or aged ICR mice were purchased from Japan SLC, Inc. (Shizuoka, Japan). All experiments were carried out under the permission of the institutional Animal Research Committee.

Sample preparation for N-glycan analysis

A 12-week-old (12w) ICR mouse was sacrificed, and their whole brain was quickly removed and washed with ice-cold phosphate-buffered saline (PBS, pH 7.4). Tissues were homogenized in a nine-fold volume of acetone using a polytron homogenizer. After acetone precipitation, samples were dried up *in vacuo* before use.

Sample preparation for SDS-PAGE and 2D-PAGE

A 12w ICR mouse was sacrificed, their whole brain quickly removed and washed with ice-cold PBS (pH 7.4). Tissues were homogenized in a twenty-fold volume of a homogenate buffer A (20 mM Tris-HCl [pH 8.0], 2 mM EDTA and 0.32 M sucrose) using Potter-Elvehjem homogenizer. The homogenate was centrifuged at 700 g for 10 min, and supernatants were collected. The supernatants were then centrifuged at 20,000 g for 1 h, and supernatants were removed by suction. The pellet were suspended in 1 ml of lysis solution B containing 9.8 M urea, 0.5 mM EDTA, 2 % (w/v) NP-40, 100 mM DTT, 0.5 % (v/v) IPG buffer and 0.001 % (w/v) bromophenol blue (BPB) and stood for 2 h at room temperature with stirring.

Subcellular fractionation (Figure 2A)

This experiment was totally done on ice. This experiment was performed as described previously [Carlin et al., 1980]. In brief, five 12w ICR mice brains were homogenized in a four-fold volume of homogenate buffer C (10 mM Hepes-NaOH [pH 7.4] and 0.32 M sucrose containing 0.2 mg/ml phenylmethylsulfonyl fluoride (PMSF), 0.01 mg/ml leupeptin, 0.01 mg/ml pepstatin A, 1 mM N-ethylmaleimide (NEM), and 1 mM EDTA. Homogenate was centrifuged for 10 min at 1,000 g to remove crude nuclear fraction (P1). The supernatant (S1) was centrifuged at 9,000 g for 15 min to obtain a pellet (P2) and supernatant (S2). The S2 fraction was centrifuged at 100,000 g for 1 h to obtain a pellet (P3) and supernatant (S3). The P2 fraction was resuspended in the homogenate buffer B. Discontinuous sucrose gradients containing 6 ml of the resuspended P2 material and 6 ml each of 0.8, 1.0, and 1.2 M sucrose solutions in 10

mM Hepes-NaOH, (pH 7.4), were centrifuged at 58,000 g for 2 h. The band between 1.0 and 1.2 M sucrose was obtained as a synaptosomal fraction (Syn). This Syn fraction was extracted with 0.5 % (v/v) Triton X-100 in 0.16 M sucrose and 6 mM Tris-HCl (pH 8.0), and then centrifuged at 33,800 g for 20 min to divide into soluble (T-sol) and insoluble fractions (PSD). Proteins of each fraction were used for 2D-PAGE, N-glycan analysis and western blot analysis (WB).

Treatment of S2, P2, P3, and Syn fractions for N-glycan analysis

S2, P2, P3, and Syn fractions obtained from subcellular fractionation were suspended in a three-fold volume of organic solvent (methanol: chloroform 2:1) to remove lipids and the suspension was centrifuged at 10,000 g for 20 min. This procedure was repeated three times. After delipidation, the pellet was washed again with 3 ml of methanol. After removing of the supernatants, the pellet was dried up *in vacuo* before use.

Treatment of Syn fraction for 2D-PAGE

Syn fraction was treated as described previously [Ishioka et al., 1990; Nakamura et al., 2005] to apply to 2D-PAGE. Syn fraction obtained from subcellular fractionation was resuspended in a nine-fold volume of 10 mM Hepes-NaOH, (pH 7.4), and centrifuged for 2 h at 58,000 g. The supernatants were removed by suction. Then the pellet was suspended in an organic solvent (methanol: chloroform 2:1) and the suspension was centrifuged at 10,000 g for 20 min. This procedure was repeated three

times. After delipidation, the pellet was washed again with 3 ml of methanol followed by washing with 3 ml of 50 mM phosphate buffer. Finally, the pellet was resuspended in 1 ml of lysis solution D containing 5 M urea, 2 M thiourea, 2 % (w/v) CHAPS, 2 % (w/v) SB-10, 2 % (v/v) IPG buffer, 60 mM DTT, 0.0025 % (w/v) Orange G and stood for 1-2 h at room temperature with stirring. Seven hundred μg of proteins were used for 2D-PAGE.

SDS-PAGE and WB

Equal volumes of the harvested proteins were applied to SDS-PAGE using 10 % polyacrylamide gel and separated electrophoretically with a Tris-glycine buffer (0.025 M Tris, 0.192 M glycine, 0.1 % SDS). Gels were then applied to Coomassie Brilliant Blue (CBB) staining or immunoblotting. For immunoblotting, separated proteins were transferred to a PVDF membrane with a semidry blotting apparatus (ATTO Corporation, Tokyo, Japan) at 240 mA for 2 h at 4℃ using buffer containing 192 mM glycine, 100 mM Tris, 5 % methanol. In some experiments, the protein spots on the 2D-PAGE gels were also electro blotted onto a PVDF membrane as described above. The membrane was then blocked with 0.5 % (w/v) skim milk in PBS containing 0.1 % (w/v) Tween-20 for 1 h at room temperature. The membrane is treated with first antibodies, CRT, PSD95, GM130, and TfR for over night at 4 ℃. The membrane was then treated with HRP conjugated anti-mouse or rabbit IgG for 1 h at room temperature. Immunoreactive spots were detected using an enhanced chemiluminescence detection kit (ECL plus).

2D-PAGE

Mouse brain homogenate and Syn fraction were prepared for 2D-PAGE. This experiment was performed as described previously [Ishioka et al., 1990; Nakamura et al., 2005]. The isoelectric focusing (IEF, first dimension) was carried out on nonlinear immobilized pH gradients (pH 3-11). Placing the IPG strips gel side down in a rehydration tray that contains the 700 μg of proteins in an appropriate rehydration solution for 14-16 h to perform passive sample application during dehydration. As the strips hydrated, proteins were absorbed and distributed over the entire length of the strip. The IEF was performed at 20 ℃ using Ettan IPGphor II (GE Healthcare) with the following two voltage programs: 500 V for 4 h, 1000 V for 1h, 8000 V for 6 h (program A for a brain homogenate) or 500 V for 2 h, 700 V for 1 h, 1000 V for 1h, 1500 V for 1 h, 2000 V for 1 h, 2500 V for 1 h, 3000 V for 1 h, 3500 V for 18 h (program B for a synaptosome). After completion of electrofocusing, IPG strips were equilibrated for 30 - 45 min in 6 M urea, 30 % glycerol, 2 % (w/v) SDS, 0.025 M Tris-HCl (pH 6.8), 0.325 M DTT. Then IPG strips were treated with 30 % glycerol, 2 % (w/v) SDS, 0.025 M Tris-HCl (pH 6.8), 4.5 % (w/v) iodoacetoamide. In the second-dimensional SDS-PAGE, the equilibrated IPG strip was placed on top of the 10 % polyacrylamide gel and proteins on the strip were separated electrophoretically. Gels were then applied to CBB-staining, silver-staining (Silver Stain MS Kit, Wako, Japan) and immunoblotting.

Liquid chromatography-mass spectrometry (LC-MS)

Protein spots on the CBB or silver-stained 2D-PAGE gel were excised by a

razor. The excess dye of CBB was removed from the gel pieces by immersing in 50 % (v/v) acetonitrile and 25 mM ammonium bicarbonate, further dehydrated in absolute acetonitrile, and dry up. The excess dye of silver-staining was removed with Silver Stain MS Kit according to the manufacturer's protocol. Then gel pieces were treated with reducing solution (10 mM DTT, 25 mM ammonium bicarbonate) and alkylating solution (1 % (w/v) iodoacetamide, 25 mM ammonium bicarbonate), and finally dehydrated in absolute acetonitrile, followed by dring up. Proteins in gel pieces were digested with 10 μg/ml trypsin and 50 mM ammonium bicarbonate overnight at 37 ℃. After digestion, peptide fragments were extracted from gel pieces in 5 % (v/v) TFA and 50 mM ammonium bicarbonate. Peptide fragments in supernatants were subjected to LC-MS.

Proteolytic peptides were separated by reversed-phase columns, packed nano-capillary column (NTCC-360/75-3, Nikkyo Technos Co. Ltd., Tokyo, Japan) with a EASY-nLC system (pump A with 0.1 % formic acid and pump B with 0.1 % formic acid in acetonitrile). For analysis of peptides, separation was performed with a linear gradient from 0 to 80 % pump B over 12 min at a flow rate of 0.3 μl/min, and mass spectra were recorded with a Orbitrap Elite system (Thermo Fisher Scientific) using a scan event (m/z 350-2000). LC-MS was performed using a capillary voltage of 1.7 kV and a capillary temperature of 250 °C. LC-MS data were analyzed with Mascot ver.2.5.1 (Matrix science, London, UK) and Proteome Discoverer software (Thermo Fisher Scientific). LC-MS analysis was supported by Functional Genomics Facility, NIBB Core Research Facilities.

Hydrazinolysis

Hydrazinolysis was performed as described previously [Tanabe and Ikenaka, 2006]. Lyophilized samples were heated with 200 μl of anhydrous hydrazine at 100 ℃ for 10 h in a water bath.

In-gel hydrazinolysis method

In-gel hydrazinolysis was performed as described previously [Yoshimura et al., 2012]. Samples were subjected to a SDS-PAGE or 2D-PAGE followed by CBB staining. Target protein bands or spots were excised from gels, and the excised gels were cut into small (4 mm height x 4 mm width x 2mm depth) pieces. Gel pieces were transferred to 5-ml glass tubes with screw caps and were washed with 1 ml of ultrapure water. The water was then removed by suction, and the gels were treated with 400 μl of 100 % methanol for 5 min. The methanol was then removed by suction and the gels were lyophilized. Glass tubes containing gels were then heated with 300 μl of anhydrous hydrazine at 100 ℃ for 10 h in a water bath. The hydrazine solution was mixed with 1ml of 10 mM ammonium bicarbonate buffer, and sugar chains were extracted by sonication for 10 min. This step was repeated three times for efficient sugar chain extraction.

N-Glycan purification and in-column reacetylation by a graphite carbon column

N-Glycan purification and in-column N-acetylation was performed as described previously [Tanabe and Ikenaka, 2006]. A graphite carbon column was

washed with 6 ml of solution I (50 mM triethylamine acetate buffer [pH 7.0] and 60 % (v/v) acetonitrile) and 6 ml of 50 mM ammonium acetate buffer (pH 7.0) for column preparation. The hydrazinolyzed sample solution was then loaded onto the graphite carbon column. After the column was washed with 6 ml of 50 mM ammonium acetate buffer for two times, the sugar chains were eluted with 5 ml of solution I with 100 μl of acetic anhydride at room temperature. The eluted solution was dried using a centrifugal concentrator, and the N-acetylated glycans were collected.

Pyridylamine derivatization

The reducing ends of the liberated glycans were tagged with the fluorophore (2-AP) as described previously [Hase et al.,1978; Hase et al., 1981; Natsuka and Hase, 1998]. After in-column removal of hydrazine and N-acetylation of glycans, the dried glycans were heated with 20 μl of a 2-AP solution (prepared by mixing 50 μl of acetic acid and 138 mg of 2-AP) at 90 ℃ for 1 h. The Schiff base was reduced by heating with 70 μl of a dimethylamine borane solution (freshly prepared by mixing 50 μl of ultrapure water, 80 μl of acetic acid, and 200 mg of dimethylamine borane) at 80 ℃ for 35 min.

N-Glycan purification by a cellulose column

Excess reagents were removed using a cellulose column according to the manufacturer's instructions with minor modifications. A cellulose column was washed with 6 ml of solution II (1-butanol: ethanol: 0.6 M acetic acid 4:1:1, v/v) for column preparation. The PA-N-glycans were mixed with 2.5 ml of solution II and loaded onto

the cellulose column. After two washes with 3 ml of solution II, the PA-N-glycans were eluted with 2 ml of solution III (75 mM ammonium bicarbonate solution: ethanol 2:1, v/v) at room temperature. The eluted solution was dried using a centrifugal concentrator.

Neuraminidase treatment and collection of neutral N-glycans

Purified PA-N-glycans were treated with neuraminidase (Nacalai Tesque, Inc.) or α2,3-sialidase (New England Biolabs, Inc.) at 37 ℃ for 14 h to cleave sialic acids, followed by heating at 100 ℃ for 5 min and filtering through a 0.20 μm spin filter (Ultrafree-MC LG, Merk Millipore). To separate neutral N-glycans from acidic ones, PA-N-glycans were passed through an anion exchange (DEAE) column (TSKgel DEAE-5PW, Tosoh, Tokyo, Japan) using high performance liquid chromatography (HPLC) or a Microgranular DE52-packed column (Whatman, GE Healthcare). Water adjusted to pH 9.0 with ammonia was used as a mobile solvent. Neutral N-glycans were collected in the nonadsorbed fraction.

N-Glycan analysis by HPLC

PA-N-glycans of varying sizes were separated by HPLC using a normal-phase (NP) column (Shodex Asahipak NH2P-50 4E, 4.6_250 mm, Showa Denko K.K., Tokyo, Japan) at a flow rate of 0.6 ml/min at 30 ℃. The mobile phase consisted of solvent A (93 % acetonitrile and 0.3 % acetic acid titrated to pH 7.0 with 1 M aqueous ammonia) and solvent B (20 % acetonitrile and 0.3 % acetic acid titrated to pH 7.0 with 1 M

aqueous ammonia). The column was equilibrated with mixtures of solvent A and solvent B (80:20) that were linearly increased to 49 % in 240 min and then to 90 % in 7 min. NP column HPLC was performed using the Prominence HPLC system equipped with a fluorescence detector (excitation and emission wavelengths were 310 and 380 nm, respectively, Shimadzu, Kyoto, Japan) or Gilson HPLC system (excitation and emission wavelengths were 310 and 380 nm, respectively, Gilson, Middleton, WI, USA). Each detected PA-Nglycan was further analyzed by reverse phase (RP) column HPLC. RP column HPLC was performed on the AQUITY UPLC system (Waters, Milford, MA, USA) using ACQUITY UPLC BEH C18 1.7 μm column (2.1 x 50 mm, Waters) at a flow rate of 0.3 ml/min at 35 ℃. Solvent C consisted of 5 mM ammonium acetate buffer (pH 4.0), and solvent D consisted of solvent C containing 10 % acetonitrile. The column was equilibrated with a mixture of solvent C and solvent D (initially 5 % D) that were increased linearly to 33 % in 11 min and then to 70 % in 1 min. PA-sugar chains were detected at excitation and emission wavelengths of 320 and 400 nm, respectively (Waters).

Data quantification and analysis

NP column HPLC chromatogram data were analyzed with LC station software (Shimadzu), Unipoint software (Gilson). RP column HPLC chromatogram data were analyzed with Empower2 software (Waters).

Immunocytochemistry of cortical neuron culture and counting of spine number

Cultured cortical neurons (0.5 x 10^5 cells / cm^2) were seeded onto 12-mm cover slips in 4-well dishes. Neurons (12DIV) were transfected with N2-EGFP vector by Lipofectamine 2000. Five days after transfection, neurons were fixed with 4 % paraformaldehyde (PFA) in 0.1 M PBS (pH 7.4) at room temperature for 10 min, and treated with -20 ℃ methanol for 10 min. The neurons were then blocked with PBS containing 10 mg/ml BSA for 1 h at room temperature. The neurons were treated with first antibodies, against PSD95 and CRT for over night at 4 ℃. Alexa 568-conjugated anti-rabbit IgG or Cy5-conjugated anti-mouse IgG was used as a secondary antibody. Samples were observed by confocal laser scanning microscopy system (TCS SP5 II: Leica Microsystems GmbH, Wetzlar, Germany). We randomly chose sixteen GFP-expressing neurons from eight separate cultures and obtained an image of dendrite from each neuron by LAS AF software (Leica Microsystems). To quantify the spine number, each image was reconstructed by a z-series maximal projection of 5-8 images, taken at 0.5 μm depth intervals. The number of spines labeled by anti-PSD95 antibody and/or anti-CRT antibody (threshold for CRT was set at 2500 to 300 arbitrary units of mean fluorescent intensity) was counted. Finally, the ratio of PSD95-CRT-positive spines to PSD95-positive spines was calculated. Box-and-whisker plots are shown to identify the median, 25th, and 75th percentiles.

Surface plasmon resonance (SPR) analysis

SPR was measured by Biacore 3000 or Biacore X100 at 25 °C (GE Healthcare). Fc and Siglec-H-Fc, recombinant protein (kindly provided by Dr. Konishi

in Nagoya university) was diluted to 1-2 μM with 10 mM sodium acetate (pH 4.5) and immobilized to the flow cells of CM5 sensor chip (GE Healthcare) using an amine-coupling kit (GE Healthcare) at a flow rate of 10 μl/min for 7 min. The immobilization level was 3666-4944 and 13370-17604 resonance units for Fc and Siglec-Fc respectively. First the immobilization was confirmed by injecting 0.2 μM of rat monoclonal anti-Siglec-H antibody (#16-0333-82, eBioscience, Santa Clara, CA, USA) or isotype control antibody (Rat IgG1, #16-4031-85, eBioscience). Different concentrations of 6SLeC cluster and control sugar chain clusters (sugar chain clusters were kindly synthesized and provided by Dr. Manabe in Osaka university) in 10 mM Hepes-NaOH (pH 7.4) containing 150 mM NaCl were injected for 1 or 2 min and then dissociation was analyzed for 1 or 2 min at a flow rate of 10 μl/min. Flow cells were regenerated with 10 mM glycine-HCl (pH 3.0) after each measurement. The sensorgram are shown by subtraction of Fc-immobilized flow cell from Siglec-H-Fc-immobilized one.

Results

Structure of sialylated A2G'2F in mouse brain

Level of desialylated A2G'2F is increased during development in the mouse brain [Torii et al., 2014]. Desialylated A2G'2F and desialylated A2G2F (Figure 1A) are expressed in the 12w mouse brain at a comparable level [Ishii et al., 2007]. A2G'2F and A2G2F are composed of the same sugar residues, thus mass spectrometry is unable to distinguish these two N-glycans. On the other hand HPLC is able to distinguish A2G'2F from A2G2F by their retention time. Therefore, HPLC was chosen for my studies. A2G'2F has four sugar residues (Gal, GlcNAc), which potentially can be sialylated by sialyltransferases (Figure 1A). Previously, we detected di-, tri-sialylated A2G'2F and 6SLeC structure on di-sialylated A2G'2F in the 12w mouse brain [Torii et al., 2014]. I investigated whether there are other sialylated A2G'2Fs. Mouse brains (12w) were acetone precipitated, and N-glycans were purified from 16 mg of dried precipitate as described in Materials and Methods. N-glycans were subjected to the DEAE column HPLC, which separates glycans according to their negative charge (Figure 1B, C). Fractions corresponding to neutral N-glycan-containing fraction (N), mono-sialylated N-glycan-containing fraction (Sia-1), di-sialylated N-glycan-containing fraction (Sia-2), and so on were isolated (Figure 1C). A peak between N and Sia-1 was derived from contaminants that could not be removed during N-glycan purification. The N fraction was collected and N-glycans in the N fraction were directly subjected to the normal phase (NP) column HPLC to separate glycans according to their molecular weight

(MW). To characterize the sialylated A2G'2F, Sia-1, Sia-2, Sia-3, and Sia-4, which contains sialylated N-glycans, were treated with α2,3-sialidase to remove α2,3-linked sialic acids, and were subjected again to the DEAE column HPLC. As an example, chromatogram of α2,3-sialidase-treated Sia-3 subjected to the DEAE column HPLC is shown in Figure 1D. Fractions corresponding to neutral N-glycan-containing fraction (Sia-3-n), mono-sialylated N-glycan-containing fraction (Sia-3-s1), di-sialylated N-glycan-containing fraction (Sia-3-s2) and so on were isolated (Figure 1D). Then peaks were treated by neuraminidase to remove all sialic acids. Neuraminidase-treated fractions were subjected to the NP column HPLC to separate glycans according to their MW (an example for Sia-3-s1 fraction treated with neuraminidase is shown in Figure 1E). The A2G'2F-containing Fraction A of neuraminidase-treated Sia-3-s1 was collected. Fraction A still contained various N-glycans. To separate each N-glycan, Fraction A was subjected to the reverse phase (RP) column HPLC (Figure 1F). Peak pointed by an arrow showed the same elution time as the standard, A2G'2F. Therefore, A2G'2F was detected in Fraction A (Figure 1F, arrow). Similar experiments were performed with Sia-1, Sia-2 and Sia-4. α2,3-linked sialic acids never attaches to the GlcNAc residue in the type 1 antennary [Galβ(1-3)GlcNAc-] of N-glycans. Furthermore, we have previously shown that di-sialylated A2G'2F contained two [Galβ(1-3){NeuAcα(2-6)}GlcNAc-] structures [Torii et al., 2014]. From the present and previous studies, structures of sialylated A2G'2Fs were determined (Table 1). In addition to our previous studies, detailed structure of tri- and tetra-sialylated A2G'2F were determined. This result indicates that there are many sialylated A2G'2Fs in a

mouse brain.

Detection of A2G'2F in subcellular fractionated proteins

N-glycosylation occurs in the ER and Golgi apparatus during transportation of proteins to the cell surface. To understand A2G'2F localization in cells of a mouse brain, subcellular fractionation of 12w mice brain was performed as described in Materials and Methods (Figure 2A). S1 fraction was separated into S2 and P2 fraction. P2 fraction contains membrane proteins. S2 fraction was separated into S3 and P3 fractions. S3 fraction contains cytosolic proteins and P3 fraction contains proteins in the ER and Golgi apparatus. Syn fraction was obtained by sucrose density gradient centrifugation of the P2 fraction. N-glycans were purified from proteins in S2, P2, P3, and Syn fractions. I found that there were various types of sialylated A2G'2Fs in the mouse brain (Table 1) and thus it is difficult to identify each sialylated A2G'2F by our HPLC system from a trace amount of sample such as subcellular fractionated proteins. Thus, all sialic acids of sialylated N-glycans were removed by neuraminidase and total desialylated A2G'2F was detected. Relative abundance of A2G'2F in these fractions were calculated (Figure 2B). A2G'2F was detected in all fractions but it was accumulated in the P2 and Syn fraction (Figure 2B). This result suggests A2G'2F mainly locates on a cell membrane and synapses.

Detection of candidate proteins for the A2G'2F-carrier

Membrane proteins carry N-glycans and express them on a cell surface.

A2G'2F is the major type 1 N-glycan in the mouse brain [Torii et al., 2014]. Thus identification of A2G'2F-carriers become synonymous with that of 6SLeC-carriers. First I studied whether A2G'2F was carried on various proteins or not. Mouse brain (12w) was homogenized, and proteins were fractionated as described in Materials and Methods. Then 700 μg of proteins were separated by a SDS-PAGE. The gel was stained with CBB to detect proteins and cut into 20 pieces (Figure 3A). N-glycans were purified from each gel piece by the direct hydrazinolysis [Yoshimura et al., 2012], and N-glycans were treated with neuraminidase to remove sialic acids. N-glycans were subjected to the DE52 column to fractionate neutral N-glycans. Neutral N-glycans were subjected to the NP column HPLC and A2G'2F-containing Fraction B was collected (Figure 3B). Then Fraction B was subjected to the RP column HPLC and A2G'2F was detected (Figure 3C). N-glycans were detected in all gel pieces (Figure 3Da), whereas A2G'2F was detected in gel #1 to 9 (Figure 3Db). Gel #7 and #8 contained high ratio of A2G'2F against total N-glycans (Figure 3Dc). This result indicates the majority of A2G'2F-carriers are 50-70 kDa proteins.

To further purify A2G'2F-carriers, the same mouse brain homogenate sample was subjected on a 2D-PAGE. Many spots of proteins were detected by CBB staining and 50-70 kDa protein spots were separated into 10 areas (Figure 4A). N-glycans were purified and analyzed as described above. A2G'2F was detected only in gel b (Figure 4Bb). A2G'2F was not detected in the adjacent gel pieces, gel a and c (Figure 4Ba, c). This result indicates that A2G'2F is carried abundantly on restricted proteins.

A2G'2F accumulated in the Syn fraction (Figure 2B). Thus proteins in the

Syn fraction were separated by 2D-PAGE and gel pieces in a similar area to gel b were excised, but into 5 pieces (Figure 4Ca, b). A2G'2F was detected in all gel pieces (Figure 4Da). To identify A2G'2F carrier proteins, gel was silver-stained and proteins in the same gel pieces were identified by a LC-MS. Among many identified proteins, N-glycan structure on neurotrimin (NTM) and limbic system-associated membrane protein (LAMP) in adult rat brain were reported [Itoh et al., 2008]. There is a N-glycan whose sugar chain structure was consistent with A2G'2F on NTM, but not on LAMP. In this report the linkage between the residues was not determined, so the structure was not completely determined. Thus NTM is a strong candidate as the A2G'2F-carrier. LC of the LC-MS detects peptides of digested proteins. The average area of largest three peptide peaks of each protein was calculated by Proteome Discoverer software (Figure 4Db, c). NTM was detected in all gel pieces, similar to A2G'2F. However, the pattern of average area of this proteins did not match with that of the A2G'2F (Figure 4Da, b). This result suggests that there are other A2G'2F-carriers than NTM in 12w mouse brain. CRT were considered to be the additional candidate as the A2G'2F-carrier by following three reasons: 1) CRT showed the highest score that is calculated by Mascot in gel i. 2) CRT has amino acid consensus sequence (Asn-X-Ser/Thr) for N-glycan modification. 3) the cellular localization of each protein is consistent with my results (Table 2). The pattern of average area in CRT after the 2D-PAGE was different from that of NTM (Figure 4Db, c). From these results, it is suggested that NTM and CRT are candidates for A2G'2F-carriers in the 12w mouse brain.

Syn fraction was extracted with Triton X-100, and then centrifuged to divide

into T-sol (soluble) and PSD (insoluble) fractions. Then 700 μg of proteins were separated by a SDS-PAGE. The gel was stained with CBB to detect proteins and gel containing 50-70 kDa protein was cut into 3 pieces (Figure 5A). N-glycans were purified from each gel piece by the direct hydrazinolysis [Yoshimura et al., 2012], and were treated with neuraminidase to remove sialic acids. N-glycans were then subjected to DE52 column to fractionate neutral N-glycans. Neutral N-glycans were subjected to the NP column HPLC and A2G'2F-containing Fraction C was collected (Figure 5B). Then Fraction C was subjected to the RP column HPLC to detect A2G'2F (Figure 5C). Gel IV and V contained high ratio of A2G'2F against total N-glycans (Figure 5D), whereas gel VII and VIII contained low ratio of A2G'2F. This result indicates that A2G'2F is mainly accumulated in Triton X-100-soluble component of the synaptosomal fraction. CRT in the P3, T-sol, and PSD fractions was detected by the WB (Figure 5A). CRT was detected in the P3 (between gel I and II) and T-sol (between gel IV and V) fraction but not in the PSD fraction. This result also indicates that CRT is a candidates for A2G'2F-carriers.

WB of subcellular fractionated samples

Previous studies show that NTM is expressed in neuron and plays a role in development and stabilization of synapses [Gil et al., 1998; Gil et al., 2002; Hashimoto et al., 2009; McNamee al., 2002; Sanz et al., 2015]. CRT is known as a chaperone protein in ER [Nauseef et al., 1995; Peterson et al., 1995]. However, recent studies also showed that it is also expressed on the cell surface [Arosa et al., 1999; White et al.,

1995]. To understand localization of CRT in the mouse brain, WB of subcellular fractionated samples were performed. Strong signal of GM130, which is the Golgi apparatus marker, was detected in P3, whereas postsynaptic density protein PSD95 was detected in the PSD fraction (Figure 6A). These results showed that the subcellular fractionation was complete. CRT was detected in the Homo S1-3, P1-3, Syn and T-sol fractions (Figure 6A). CRT is a chaperon in the ER and hence it was mainly contained in the P3 fraction. CRT was also detected in the Syn and T-sol fraction. The result of WB of CRT was similar with that of TfR (Figure 6A). TfR is contained in recycling endosome and mainly expressed in the P3 fraction, whereas a part of it is also present in synapses but not in postsynaptic density. This result indicates that CRT is expressed not only in ER but also in synapses outside the postsynaptic density, like TfR. CRT was detected in gel pieces of the 2D-PAGE-separated Syn fraction by LC-MS (Figure 4Dc). Thus this protein should be detected in the same area of gel pieces by WB. Proteins in the Syn fraction was separated by 2D-PAGE and these were transferred on PVDF membrane. CRT was detected by WB (Figure 6B). After the WB, membrane was stained by CBB. Multiple comparisons between the results of the WB (Figure 6Ba), CBB stained membrane (Figure 6Bb) and CBB stained gel for LC-MS (Figure 4C) were performed (Figure 6Bc, d, e). The signal of CRT was detected in gel i and v (Figure 6Be). A high amount of CRT was detected in gel i and v by the LC-MS. These results indicate that the result of the WB fits well with that of the LC-MS.

Immunocytochemistry of CRT in GFP-expressing neurons

WB of CRT indicates that this protein was expressed in the synapse of 12w mouse brain (Figure 6A). To confirm localization of CRT in neurons, cortical neurons from E16 mice brain were cultured. They were transfected with expression vector encoding EGFP at 12 DIV. At 17 DIV, neurons were fixed and immunostained by anti-CRT and anti-PSD95 antibody. CRT was mainly expressed in the cell body (Figure 7A) and dendrites. Furthermore, some of CRT was observed in spines (Figure 7Bi, ii). Signals of CRT were detected in about 10 % of PSD95-positive spines and these were apposed to signals of PSD95 (Figure 7C). This result suggests that CRT is expressed in mature synapses outside the postsynaptic density.

The interaction between 6SLeC and siglec-H

Sialylated N-glycans are localized on the cell surface and interact with other cells through siglec. So far, no mouse siglecs other than siglec-E are known to interact with 6SLeC structure. Siglec-H is up regulated in activated microglia in the mouse brain [Kopatz et al., 2013], and the ligand glycan structure for siglec-H is unknown. Thus, I focused on siglec-H. To investigate whether 6SLeC interacts with siglec-H or not, SPR was performed. The affinity of sugar chain to protein is weaker than that of the protein to protein interaction (1/100-1/10,000). Thus, it is difficult to observe interaction between proteins and glycans by Biacore assay. To overcome this problem, I newly chose “sugar chain cluster” as analyte for this assay [Tanaka et al., 2010]. In lipid rafts, the affinity of sugar chain for protein becomes stronger by clustering of sugar chains [Taniguchi et al., 2008]. Sugar chain cluster increases local concentration of sugar

chains like lipid rafts, thus it must be able to increase the affinity of sugar chains for proteins. Sugar chain clusters harboring 6SLeC or control sugar chain clusters were kindly synthesized and gifted by Dr. Manabe in Osaka University (Figure 8A). Dr. Konishi in Nagoya University supported to perform Biacore assay. Siglec-H was immobilized on the sensor chip and then analyte sugar chain clusters were injected into Biacore. A response, which reflects an interaction between siglec-H and sugar chain clusters, was observed when 6SLeC cluster (Figure 8Ab) was injected, whereas it was not observed when sialylated or non-sialylated A2G2 cluster (Figure 8Ad, e, f) was injected (Figure 8B). This result indicates that siglec-H interacted with 6SLeC [Galβ(1-3){NeuAcα(2-6)}GlcNAc-] but not with [NeuAcα(2-6/2-3)Galβ(1-4)GlcNAc-] structure. A response of 6SLeC cluster and siglec-H interaction was weaker than that of anti-siglec-H antibody and siglec-H interaction (Figure 8B, C). This is because of the low MW of sugar chain cluster. Amplitude of response depends on the size of analytes. The MW of sugar chain cluster is about 25 kDa, whereas that of antibody is about 150 kDa. Thus, response of anti-siglec-H antibody and siglec-H interaction should be six times bigger than that of 6SLeC cluster and siglec-H interaction.

To investigate whether siglec-H recognizes a sialic acid on 6SLeC or not, 6SLeC cluster or LewisC (LeC) cluster (Figure 8Ab, c) was injected to Biacore. 6SLeC cluster interacted with siglec-H, whereas LeC cluster did not interacted with siglec-H (Figure. 8D). The dose dependence of interaction between siglec-H and 6SLeC was also observed (Figure 8E). These results indicate siglec-H properly distinguish sialic

acid on 6SLeC.

Discussion

Possible recognition of synapse by microglia through 6SLeC-containing N-glycans

I tried to reveal the role of 6SLeC through the interaction with 6SLeC-recognizing siglec in the adult mouse brain. First, I applied our improved method [Yoshimura et al., 2012] to determine the N-glycan structure from glycoproteins in the SDS- or 2D-PAGE gels (Figure 2, 3, 4, 5). My results showed that sialylated A2G'2F is not carried ubiquitously by glycoproteins but rather by a restricted number of acidic proteins with molecular mass of 50-70 kDa mainly present in the Triton X-100-soluble component of the synaptosomal fraction. NTM and CRT were strong candidates as A2G'2F-carriers. NTM was present as a main glycoprotein in the gel pieces with abundant A2G'2F-carrying proteins and was reported to carry a N-glycan whose structure is consistent with the 6SLeC-containing A2G'2F [Itoh et al., 2008]. A2G'2F was abundantly present in the gel pieces with low NTM content. In these gel pieces CRT was the most abundant glycoprotein. I revealed that CRT was expressed not only in the ER, but also at the plasma membrane and a portion of synapses by using immunohistochemistry and biochemical experiments (Figure 6, 7). I showed A2G'2F was accumulated in the P2 and Syn fraction (Figure 2B). My results and previous studies suggest that sialylated A2G'2Fs may be transported to the plasma membrane of neuron (synapse) by glycoproteins, such as NTM and CRT. I tried to detect A2G'2F from immunoprecipitated CRT but this experiments failed because of too small amount of this protein (data not shown).

Microglia is known to express siglec-E and H. Siglec-E binds not only to α2,3- and α2,8-sialylated glycans but also to 6SLeC [Redelinghuys et al., 2011]. Ligands for this siglec-H have not been determined. I chose sugar chain cluster as a ligand for Biacore assay to improve the strength of interaction between sugar chains and proteins. I observed that 6SLeC bound to siglec-H (Figure 8).

My studies revealed an interaction between 6SLeC and siglec-H. I also revealed that CRT is a novel candidate for sialylated A2G'2F-carrier. Since CRT was found to be present in a subpopulation of synapse and siglec-H is expressed by microglia, this interaction may be involved in recognition of synapse by microglia.

Hypothesis for the role of 6SLeC-siglecs interaction

Here, I describe my hypothesis for the role of 6SLeC-containing sialylated A2G'2F on cell-cell interaction in the mouse brain (Figure 9). Sialylated N-glycans are abundant on the neuronal surface by membrane proteins, like NTM and CRT. Siglec-E binds to α2,3- and α2,8-sialylated glycans, and 6SLeC. Siglec-E inhibits microglial phagocytosis of healthy neurons through inhibition signaling. Furthermore, siglec-E binds to 6SLeC and may prevent it from recognition by siglec-H. Desialylation is one of the mechanisms for inducing phagocytosis by immune cells [Li et al., 2015; Meesmann et al., 2010; Seyrantepe et al., 2010; Watanabe et al, 2004]. When condition of neurons is changed such as apoptosis, malignant transformation etc., the amount of 6SLeC-containing sialylated A2G'2F increase as a result of increased transfer of α2,6-linked sialic acids by highly-expressed sialyltransferases and removal of α2,3- and

α2,8-linked sialic acids by neuraminidases. Interaction between 6SLeC and siglec-H was not observed when 6SLeC monomer was used (data not shown). These results suggest siglec-H binds to increased and clustered 6SLeC-containing sialylated A2G'2F in abnormal neuronal conditions.

NTM is expressed in neurons including synapses and mediates synaptogenesis [Gli, 2002; Hashimoto, 2009]. NTM is involved in synaptogenesis of hippocampal neurons in vitro [Hashimoto et al., 2009]. The major function of CRT is chaperoning of proteins in ER [Peterson et al., 1995], but in addition, CRT localizes on the cell surface and plays a role as 'eat-me' signal in phagocytosis of apoptotic cells [Ogden et al, 2001; Obeid et al., 2007; Vandivier et al., 2002]. Furthermore, CRT-induced phagocytosis of viable neurons by activated microglia was reported [Fricker et al., 2012]. CRT has one consensus sequence for N-glycosylation site, on which various types of N-glycan are reported [Denning et al., 1997]. Thus CRT in mouse brain may be N-glycosylated and carry A2G'2F.

Siglec-H is expressed by microglia in the mouse brain [Gautier et al., 2012]. Function of siglec-H depends on the immunoreceptor tyrosine-based activation motif (ITAM)-containing adaptor protein DAP12 (TYROBP) [Blasius et al., 2006]. DAP12-signaling receptors facilitate phagocytic clearance of apoptotic cell or cellular debris [Gaikwad et al., 2009; Linnartz et al, 2012; Takahashi et al, 2005]. Siglec-H is highly expressed on activated microglia and binds to glioma cells [Blasius et al., 2013]. Thus authors concluded that activated microglia could engulf glioma cells via siglec-H-DAP12 signaling. In contrast to siglec-H, siglec-E inhibits the microglial

phagocytosis via immunoreceptor tyrosine-based inhibition motif (ITIM) and shows neuroprotective effect [Claude et al., 2013]. Binding specificities of siglec-H and siglec-E are slightly different from each other although both binds to 6SLeC: Siglec-E also binds to α2,3-linked NeuAc-Gal residues while siglec-H does not (Figure 8 and [Redelinghuys et al., 2011]). These changes in sialylation status can be achieved by extracellular neuraminidases in vivo. This might induce change in properties of microglia from protective to phagocytotic. Also two candidate carrier proteins of 6SLeC-containing sialylated A2G'2F, NTM (synaptogenesis) and CRT (induction of phagocytosis), are present on the synaptic membrane (excluding the postsynaptic density) and may play complementary roles in synapse maintenance or elimination.

Predicted biosynthetic pathway of 6SLeC-containing sialylated A2G'2F

Various type of sialylated A2G'2Fs (Figure 1, Table 1) are synthesized in the Golgi apparatus and most of them locate on the plasma membrane and synapses (Figure 2). However, the biosynthetic pathway of 6SLeC-containing sialylated A2G'2F still remains elusive. ST3GalI-VI are member of Gal α2,3-sialyltransferase family which transfer sialic acid to Gal residues . ST3GalIII prefer type 1 antennary to type 2 antennary [Kono et al., 1997]. ST6GalNAcI-VI are member of GalNAc α2,6-sialyltransferase family which transfer sialic acid to GalNAc and GlcNAc residues. Sialyl-LeC [NeuAcα(2-3)Galβ(1-3)GlcNAc-] is a substrate for ST6GalNAcV [Tsuchida et al., 2003]. mRNA expression of ST6GalNAcV was the highest of six ST6GalNAcs [Ishii et al., 2007]. I also observed strong mRNA expression of

ST6GalNAcV in the adult mouse brain by using in situ hybridization (data not shown). ST6GalNAcV expression changes the character of glioma and breast cancer cell [Bos et al., 2009; Kroes et al, 2010]. I predicted biosynthetic pathway of 6SLeC-containing sialylated A2G'2F from previous studies (Figure 9). At first, ST3Gals transfers sialic acid to terminal Gal residue through α2,3-linkage. Next, sialyl-LeC is recognized by ST6GalNAcV, followed by transfer of sialic acid to GlcNAc residue through α2,6-linkage. Finally terminal sialic acid is removed by a neuraminidase and 6SLeC is synthesized. I detected non-, mono-, di-, tri-, and tetra-sialylated A2G'2F in the adult mouse brain (Figure 1, Table 1). These structures were consistent with my prediction. Patterns of sialylation can also be changed by removing sialic acids by neuraminidases present extracellularly. In fact, neuraminidase 1 (Neu 1) localizes on the plasma membrane of the brain cells and remove sialic acid [Bonten et al., 1996; Dridi et al., 2013; Smutova et al, 2014]. Therefore, structure of sialylated A2G'2Fs can be diversified through de novo synthesis and by neuraminidases extracellularly. Thus the sialylation status of A2G'2F on the synaptic membrane should be highly dynamic and affects the interaction by siglec-E or H.

In conclusion, my results indicated a new cell-cell interaction pathway through 6SLeC-siglec-H interaction. This is the first report describing the ligand for siglec-H. This interaction may contribute to the functions of microglia. In addition, N-glycan analysis from the 2D-PAGE gel and Biacore assay using sugar chain cluster

were successful. These methods will provide more detail understanding of the N-glycan-carrier proteins and sugar chain-recognizing proteins.

References

Arosa FA, de Jesus O, Porto G, Carmo AM, de Sousa M, Calreticulin Is Expressed on the Cell Surface of Activated Human Peripheral Blood T Lymphocytes in Association with Major Histocompatibility Complex Class I Molecules. The Journal of Biological Chemistry, 274, (1999), 16917-22

Atkinson PH, Lee JT, Co-translational Excision of a-Glucose and α-Mannose in Nascent Vesicular Stomatitis Virus G Protein. The Journal of Cell Biology, 98, (1984), 2245-9

Blasius AL, Cella M, Maldonado J, Takai T, Colonna M, Siglec-H is an IPC-specific receptor that modulates type I IFN secretion through DAP12. Blood, 107, (2006), 2474-6

Bonten E, van der Spoel A, Fornerod M, Grosveld G, d'Azzo A, Characterization of human lysosomal neuraminidase defines the molecular basis of the metabolic storage disorder sialidosis. Genes & Development, 10, (1996), 3156-69

Bos PD, Zhang XH, Nadal C, Shu W, Gomis RR, Nguyen DX, Minn AJ, van de Vijver MJ, Gerald WL, Foekens JA, Massagué J, Genes that mediate breast cancer metastasis to the brain. Nature, 459, (2009), 1005-9

Carlin RK, Grab DJ, Cohen RS, Siekevitz P, Isolation and Characterization of Postsynaptic Densities from Various Brain Regions: Enrichment of Different Types of Postsynaptic Densities. The Journal of Cell Biology, 86, (1980), 831-45

Claude J, Linnartz-Gerlach B, Kudin AP, Kunz WS, Neumann H, Microglial CD33-related Siglec-E inhibits neurotoxicity by preventing the phagocytosis-associated oxidative burst. The Journal of Neuroscience, 33, (2013), 18270-6

Cylwik B, Naklicki M, Chrostek L, Gruszewska E, Congenital disorders of glycosylation. Part I. Defects of protein N-glycosylation. Acta Biochimica Polonica, 60, (2013), 151-61

Denning GM, Leidal KG, Holst VA, Iyer SS, Pearson DW, Clark JR, Nauseef WM, Clark RA, Calreticulin biosynthesis and processing in human myeloid cells: demonstration of signal peptide cleavage and N-glycosylation. Blood, (1997), 372-81

Dridi L, Seyrantepe V, Fougerat A, Pan X, Bonneil E, Thibault P, Moreau A, Mitchell GA, Heveker N, Cairo CW, Issad T, Hinek A, Pshezhetsky AV, Positive regulation of insulin signaling by neuraminidase 1. Diabetes, 62, (2013), 2338-46

Freeze HH, Aebi M, Altered glycan structures: the molecular basis of congenital disorders of glycosylation. Current Opinion in Structural Biology, 15, (2005), 490-8

Fricker M, Oliva-Martín MJ, Brown GC, Primary phagocytosis of viable neurons by microglia activated with LPS or Aβ is dependent on calreticulin/LRP phagocytic signalling. Journal of Neuroinflammation, 9, (2012)

Gaikwad S, Larionov S, Wang Y, Dannenberg H, Matozaki T, Monsonego A, Thal DR, Neumann H, Signal regulatory protein-beta1: a microglial modulator of phagocytosis in Alzheimer's disease. The American Journal of Pathology, 175, (2009), 2528-39

Gautier EL, Shay T, Miller J, Greter M, Jakubzick C, Ivanov S, Helft J, Chow A, Elpek KG, Gordonov S, Mazloom AR, Ma'ayan A, Chua WJ, Hansen TH, Turley SJ, Merad M, Randolph GJ, Immunological Genome Consortium, Gene-expression profiles and transcriptional regulatory pathways that underlie the identity and diversity of mouse tissue macrophages. Nature Immunology, 13, (2012), 1118-28

Gil OD, Zanazzi G, Struyk AF, Salzer JL, Neurotrimin Mediates Bifunctional Effects on Neurite Outgrowth via Homophilic and Heterophilic Interactions. The Journal of Neuroscience, 18, (1998), 9312-25

Gil OD, Zhang L, Chen S, Ren YQ, Pimenta A, Zanazzi G, Hillman D, Levitt P, Salzer JL, Complementary Expression and Heterophilic Interactions between IgLON Family Members Neurotrimin and LAMP. Journal of Neurobiology, 51, (2002), 190-204

Hase S, Ikenaka T, Matsushima Y, Structure analyses of oligosaccharides by tagging of the reducing end sugars with a fluorescent compound. Biochemical and Biophysical Research Communications, 85, (1978), 257-63

Hase S, Ikenaka T, Matsushima Y, A highly sensitive method for analyses of sugar moieties of glycoproteins by fluorescence labeling. The Journal of Biochemistry, 90, (1981), 407-14

Hashimoto T, Maekawa S, Miyata S, IgLON cell adhesion molecules regulate synaptogenesis in hippocampal neurons. Cell Biochemistry and Function, 27, (2009), 496-8

Ishii A, Ikeda T, Hitoshi S, Fujimoto I, Torii T, Sakuma K, Nakakita S, Hase S, Ikenaka K, Developmental changes in the expression of glycogenes and the content of N-glycans in the mouse cerebral cortex. Glycobiology, 17, (2007), 261-76

Ishioka N, Oda T, Natake Y, Kurioka S, Analysis and Separation of Synaptosomal Membrane Proteins. Neurochemical Research, 15, (1990), 475-81

Itoh S, Hachisuka A, Kawasaki N, Hashii N, Teshima R, Hayakawa T, Kawanishi T, Yamaguchi T, Glycosylation Analysis of IgLON Family Proteins in Rat Brain by Liquid Chromatography and Multiple-Stage Mass Spectrometry. Biochemistry, 47,

(2008), 10132-54

Kono M, Ohyama Y, Lee YC, Hamamoto T, Kojima N, Tsuji S, Mouse beta-galactoside alpha 2,3-sialyltransferases: comparison of in vitro substrate specificities and tissue specific expression. Glycobiology, 7, (1997), 469-79

Kopatz J, Beutner C, Welle K, Bodea LG, Reinhardt J, Claude J, Linnartz-Gerlach B, Neumann H, Siglec-h on Activated Microglia for Recognition and Engulfment of Glioma Cells. Glia, (2013), 61, 1122-33

Kroes RA, He H, Emmett MR, Nilsson CL, Leach FE 3rd, Amster IJ, Marshall AG, Moskal JR, Overexpression of ST6GalNAcV, a ganglioside-specific alpha2,6-sialyltransferase, inhibits glioma growth in vivo. Proceedings of the National Academy of Sciences of the United States of America, 107, (2010), 12646-51

Lai C, Brow MA, Nave KA, Noronha AB, Quarles RH, Bloom FE, Milner RJ, Sutcliffe JG, Two forms of 1B236/myelin-associated glycoprotein, a cell adhesion molecule for postnatal neural development, are produced by alternative splicing. Proceedings of the National Academy of Sciences of the United States of America, 84, (1987), 4337-41.

Li J, van der Wal DE, Zhu G, Xu M, Yougbare I, Ma L, Vadasz B, Carrim N, Grozovsky R, Ruan M, Zhu L, Zeng Q, Tao L, Zhai ZM, Peng J, Hou M, Leytin V,

Freedman J, Hoffmeister KM, Ni H, Desialylation is a mechanism of Fc-independent platelet clearance and a therapeutic target in immune thrombocytopenia. Nat Communications, 6, (2015), 7737

Linnartz B, Kopatz J, Tenner AJ, Neumann H, Sialic acid on the neuronal glycocalyx prevents complement C1 binding and complement receptor-3-mediated removal by microglia. The Journal of Neuroscience, (2012), 946-52

McNamee CJ, Reed JE, Howard MR, Lodge AP, Moss DJ, Promotion of neuronal cell adhesion by members of the IgLON family occurs in the absence of either support or modification of neurite outgrowth. Journal of Neurochemistry, 80, (2002), 941-8

Meesmann HM, Fehr EM, Kierschke S, Herrmann M, Bilyy R, Heyder P, Blank N, Krienke S, Lorenz HM, Schiller M, Decrease of sialic acid residues as an eat-me signal on the surface of apoptotic lymphocytes. Journal of Cell Science, 123, (2010), 3347-56

Nakamura N, Sakurai Y, Takeda Y, Toda T, Comparative proteomics of flotillin Triton X-100-insolble lipid raft fractions of mitochondria and synaptosome from mouse brain. Journal of Electrophoresis, 49, (2005), 77-83

Natsuka S, Hase S, Analysis of N- and O-glycans by pyridylamination. Methods in Molecular Biology, 76, (1998), 101-13

Nauseef WM, McCormick SJ, Clark RA, Calreticulin Functions as a Molecular Chaperone in the Biosynthesis of Myeloperoxidase. The Journal of Biological Chemistry, 270, (1995), 4741-7

Obeid M, Tesniere A, Ghiringhelli F, Fimia GM, Apetoh L, Perfettini JL, Castedo M, Mignot G, Panaretakis T, Casares N, Métivier D, Larochette N, van Endert P, Ciccosanti F, Piacentini M, Zitvogel L, Kroemer G, Calreticulin exposure dictates the immunogenicity of cancer cell death. Nature Medicine, 13, (2007), 54-61

Ogden CA, deCathelineau A, Hoffmann PR, Bratton D, Ghebrehiwet B, Fadok VA, Henson PM, C1q and mannose binding lectin engagement of cell surface calreticulin and CD91 initiates macropinocytosis and uptake of apoptotic cells. The Journal of Experimental Medicine, 194, (2001), 781-95

Peterson JR, Ora A, Van PN, Helenius A, Transient, lectin-like association of calreticulin with folding intermediates of cellular and viral glycoproteins. Molecular Biology of the Cell, 6, (1995), 1173-84

Redelinghuys P, Antonopoulos A, Liu Y, Campanero-Rhodes MA, McKenzie E, Haslam SM, Dell A, Feizi T, Crocker PR, Early murine T-lymphocyte activation is accompanied by a switch from N-Glycolyl- to N-acetyl-neuraminic acid and generation of ligands for siglec-E. The Journal of Biological Chemistry, 286, (2011), 34522-32

Sanz R, Ferraro GB, Fournier AE, IgLON Cell Adhesion Molecules Are Shed from the Cell Surface of Cortical Neurons to Promote Neuronal Growth. The Journal of Biological Chemistry, 290, (2015), 4330-42

Seyrantepe V, Iannello A, Liang F, Kanshin E, Jayanth P, Samarani S, Szewczuk MR, Ahmad A, Pshezhetsky AV, Regulation of Phagocytosis in Macrophages by Neuraminidase 1. The Journal of Biological Chemistry, 285, (2010), 206–15

Smutova V, Albohy A, Pan X, Korchagina E, Miyagi T, Bovin N, Cairo CW, Pshezhetsky AV, Structural basis for substrate specificity of mammalian neuraminidases. PLoS One, 9, (2014), e106320

Tanabe K, Ikenaka K, In-column removal of hydrazine and N-acetylation of oligosaccharides released by hydrazionolysis. Analytical Biochemistry. 348, (2006), 324-6

Tanaka K, Siwu ER, Minami K, Hasegawa K, Nozaki S, Kanayama Y, Koyama K, Chen WC, Paulson JC, Watanabe Y, Fukase K, Noninvasive Imaging of Dendrimer-Type N-Glycan Clusters: In Vivo Dynamics Dependence on Oligosaccharide Structure. Angewandte Chemie International Edition, 49, (2010), 8195-200

Tang S, Woodhall RW, Shen YJ, deBellard ME, Saffell JL, Doherty P, Walsh FS, Filbin MT, Soluble myelin-associated glycoprotein (MAG) found in vivo inhibits axonal regeneration. Molecular and Cellular Neuroscience, 9, (1997), 333-46

Takahashi K, Rochford CD, Neumann H, Clearance of apoptotic neurons without inflammation by microglial triggering receptor expressed on myeloid cells-2. The Journal of Experimental Medicine, 201, (2005), 647-57

Taniguchi N, Suzuki A, Ito Y, Narimatsu H, Kawasaki T, Hase S, Experimantal Glycoscience Glycobiology. Elsevier, (2008)

Torii T, Yoshimura T, Narumi M, Hitoshi S, Takaki Y, Tsuji S, Ikenaka K, Determination of major sialylated N-glycans and identification of branched sialylated N-glycans that dynamically change their content during development in the mouse cerebral cortex. Glycoconjugate Journal, 31, (2014), 671-83

Tsuchida A, Okajima T, Furukawa K, Ando T, Ishida H, Yoshida A, Nakamura Y, Kannagi R, Kiso M, Furukawa K, Synthesis of disialyl Lewis a (Le(a)) structure in colon cancer cell lines by a sialyltransferase, ST6GalNAc VI, responsible for the synthesis of alpha-series gangliosides. The Journal of Biological Chemistry, 278, 2003, 22787–94

Vandivier RW, Ogden CA, Fadok VA, Hoffmann PR, Brown KK, Botto M, Walport MJ, Fisher JH, Henson PM, Greene KE, Role of surfactant proteins A, D, and C1q in the clearance of apoptotic cells in vivo and in vitro: calreticulin and CD91 as a common collectin receptor complex. The Journal of Immunology, 169, (2002), 3978-86

Varki A, Cummings RD, Esko JD, Freeze HH, Stanley P, Bertozzi CR, Hart GW, Etzler ME, Essential of Glycobiology. 2nd eds, Cold Spring Harbor Laboratory Press, Cold Spring Harbor, (2009)

Vinson M, Strijbos PJ, Rowles A, Facci L, Moore SE, Simmons DL, Walsh FS, Myelin-associated glycoprotein interacts with ganglioside GT1b. A mechanism for neurite outgrowth inhibition. The Journal of Biological Chemistry, 276, (2001), 20280-5

Watanabe Y, Shiratsuchi A, Shimizu K, Takizawa T, Nakanishi Y, Stimulation of phagocytosis of influenza virus-infected cells through surface desialylation of macrophages by viral neuraminidase. Microbiology and Immunology, 48, (2004), 875-81

White TK, Zhu Q, Tanzer ML, Cell Surface Calreticulin Is a Putative Mannoside Lectin Which Triggers Mouse Melanoma Cell Spreading. The Journal of Biological Chemistry, 270, (1995), 15926-9

Yoshimura T, Yamada G, Narumi M, Koike T, Ishii A, Sela I, Mitrani-Rosenbaum S, Ikenaka K, Detection of N-glycans on small amounts of glycoproteins in tissue samples and sodium dodecyl sulfate–polyacrylamide gels. Analytical Biochemistry, 423, (2012), 253-60

Figure legends

Figure 1. Many structures of sialylated A2G'2F were detected in the mouse brain.

(A) Structure of di-sialylated A2G'2F (a). Sugar residues of desialylated A2G'2F (blue box), which are written in magenta, potentially can be sialylated by sialyltransferases, and 6SLeC (orange box) is synthesized. A2G'2F and A2G2F (b) are composed of the same sugar residues. (B) Outline of the N-glycan analysis strategy. N-glycans were purified from 12w mouse brain and labeled by pyridylamination. Enzymatic treatments and HPLC analysis of N-glycans were repeated to determine structures of sialylated A2G'2F. (C) N-glycans from 12w mouse brain were subjected to the DEAE HPLC. N, Sia-1, Sia-2, Sia-3, and Sia-4 indicate neutral, mono-sialylated, di-sialylated, tri-sialylated and tetra-sialylated N-glycans, respectively. The bars under N, Sia-1, Sia-2, Sia-3, and Sia-4 indicate fractionated eluents, respectively. * indicates non-sugar chain contamination peak. (D) Sia-3 fraction was treated by α2,3-sialidase to remove α2,3-linked sialic acid. Then α2,3-sialydase-treated Sia-3 was subjected to the DEAE column HPLC. Sia3-n, Sia3-s1, Sia3-s2, and Sia3-s3 indicate neutral, mono-sialylated, di-sialylated, and tri-sialylated N-glycans, respectively. The bars under Sia-3-n, Sia-3-s1, Sia-3-s2, and Sia-3-s3 indicate fractions collected, respectively. (E) Sia-3-s1 fraction was treated by neuraminidase to remove all sialic acid. Then neuraminidase-treated Sia-3-s1 was applied to DE52 column to purify neutral N-glycans. Neutral N-glycans were subjected to the NP column HPLC. Fraction A was collected. The bars under Fraction A indicate the fraction collected. (F) Fraction A was

subjected to the RP column HPLC. Magenta line indicates the chromatogram of Fraction A. Gray line indicates the chromatogram of A2G'2F standard. A2G'2F standard co-eluted with a peak in Fraction A (arrow), revealing that is A2G'2F peak. This experiment was performed for N-glycans contained in N, Sia-1, 2, 3, and 4, respectively.

Figure 2. A2G'2F was accumulated to P2 and Syn fraction.

(A) Outline of the subcellular fractionation. (B) N-glycans were released and purified from the S2, P2, P3, and Syn fractions and analyzed by HPLC. A2G'2F was detected by HPLCs. Peak area of A2G'2F was measured by Empower 2 software. Relative abundance of A2G'2F in four fractions were calculated. It was accumulated in P2 fraction. Significant levels; **P<0.05 vs P3 fraction (Student's t-test, p=0.049). A2G'2F also accumulated in the Syn fraction but the comparison between the P3 and Syn fraction showed no significant difference (Student's t-test, p=0.169). Data are presented as mean ±SEM of three independent experiments (n=3), **P<0.05.

Figure 3. SDS-PAGE analysis of A2G'2F-carrier proteins in the mouse brain

(A) Proteins in mouse brain homogenate (700 μg) were subjected on a 10 % SDS-PAGE. The gel was cut into 20 pieces. N-glycans were purified from each gel piece by the direct hydrazinolysis. (B) Purified N-glycans were subjected to the NP column HPLC to search for A2G'2F-containing fraction. The chromatogram of gel #7 is shown. Fraction B was collected. The bar under Fraction B indicates the fraction

collected. (C) Fraction B was subjected to the RP column HPLC to detect A2G'2F. Gray line indicates the chromatogram of A2G'2F standard. A2G'2F standard co-eluted with a peak of Fraction B (arrow), revealing that is A2G'2F peak. (D) Peak area of N-glycans in each gel piece was calculated. N-glycans were detected in all gel pieces and total area of N-glycans was measured from the result of the NP column HPLC (a). A2G'2F was abundant in gel #7 and 8 as detected by the RP column HPLC (b). The ratio of A2G'2F to total N-glycan was calculated (c). The ratio of A2G'2F was high in the gel # 7 and 8.

Figure 4. 2D-PAGE analysis of A2G'2F-carrier proteins

(A) Proteins in mouse brain homogenate (700 μg) were separated by a 2D-PAGE (1st dimension: 3-11 linear IPG strips, 2nd dimension: 10 % SDS-PAGE). The gel containing 50-70 kDa protein spots were separated into 10 pieces depending on isoelectric point of proteins. N-glycans were purified from each gel piece. (B) Purified N-glycans were subjected to the RP column HPLC. A2G'2F was detected only in gel b (b). A2G'2F was not detected even in neighboring areas such as gel a (a) and c (c). (C) Proteins in Syn fraction (700 μg) were separated by a 2D-PAGE (1st dimension: 3-11 linear IPG strips, 2nd dimension: 10 % SDS-PAGE). The similar area (a, b, white box) with gel b (c) was excised, but into 5 pieces. This experiment was repeated four times to obtain enough amounts of N-glycans for HPLC analysis. Then N-glycans were purified from each gel pieces. (D) Pattern of the content of A2G'2F, NTM, and CRT. The ratio of A2G'2F to total N-glycan was calculated (a). The average area of largest three

peptide peaks of NTM (b) or CRT (c) was calculated by Propteome Discover software. The pattern of average area of these proteins did not match with that of the A2G'2F

Figure 5. SDS-PAGE analysis of A2G'2F-carrier proteins in P3, T-sol, PSD fractions

(A) Proteins in the P3 (a), T-sol (b), and PSD (c) fraction (700 μg) were subjected to a 10 % SDS-PAGE. The gel containing 50-70 kDa protein was cut into 3 pieces (I-IX). N-glycans were purified from each gel piece by the direct hydrazinolysis. Equal volume (20 μg) of subcellular fractionated proteins was also immunoblotted using an anti-CRT antibody (1:500). Strong signal for CRT was detected in the P3 fraction, whereas CRT was also detected in the T-sol fraction. (B) Purified N-glycans were subjected to the NP column HPLC to search for A2G'2F-containing fraction. The chromatogram of T-sol gel IV is shown. Fraction C was collected. The bar under Fraction C indicates the fraction collected. (C) Fraction C was subjected to the RP column HPLC to detect A2G'2F. Gray line indicates the chromatogram of A2G'2F standard. A2G'2F standard co-eluted with a peak of Fraction C (arrow), revealing that is A2G'2F peak. (D) Peak area of N-glycans in each gel piece was calculated. N-glycans were detected in all gel pieces and total area of N-glycans was measured from the result of NP column HPLC The ratio of A2G'2F to total N-glycan was calculated. The ratio of A2G'2F was high in the gel IV and V.

Figure 6. CRT was detected in T-sol fraction.

(A) Equal volume (5 μg) of subcellular fractionated proteins was subjected to SDS-PAGE and immunoblotted using anti- PSD95 (1:1000, postsynaptic density marker), GM130 (1:200, Golgi apparatus marker), TfR (1:1000), and CRT (1:500) antibodies. Distribution of PSD95 and GM130 showed that the subcellular fractionation was complete. Strong signal for CRT was detected in the P3 fraction, whereas CRT was also detected in the Syn and T-sol fraction. The pattern of CRT was similar to that of TfR. (B) Proteins in the Syn fraction (700 μg) were separated by a 2D-PAGE (1^{st} dimension: 3-11 linear IPG strips, 2^{nd} dimension: 10 % SDS-PAGE). Separated proteins were immunoblotted by using anti-CRT antibody (a, arrow). PVDF membrane was stained by CBB (b). These two figures were merged (c). Figure 6Bc was compared with the CBB-stained gel of figure 4Ca and the result of WB (6Ba) was merged with this CBB-stained gel (d). White dot box in figure 6Bd was enlarged (e). Signal of CRT spanned from gel i to v (e, arrow).

Figure 7. CRT was detected in some portion of synapses.

(A) Immunocytochemistry of mouse cortical neurons was performed. Neurons were transfected with N2-EGFP vector at 12 DIV and immunostained using the anti-CRT (1:100) and PSD95 (1:100) antibody at 17 DIV. Some neurons expressed GFP (a, arrow). CRT was strongly expressed in the cell body of GFP-expressing neuron (b, arrow). CRT was also expressed in dendrites. Scale bar =25 μm. (B) Spines were visualized by GFP (a). Most of spines were PSD95-positive mature synapses (a, arrowheads). Some of these spines were CRT-positive (a, arrow). Signals of CRT were

apposed to that of PSD95 (Bi, ii). Scale bar =10 μm. (C) About 10 % of PSD95-positive spines were CRT-positive spines. Sixteen GFP-expressing neurons were chose randomly from eight separate cultures.

Figure 8. Siglec-H interacted with the 6SLeC cluster.

(A) Structure of sugar chain cluster. Sugar chains, such as 6SLeC, is chemically linked to 'R' (blue) on the cluster (a). One cluster contains 16 sugar chains. Sugar chain clusters were kindly synthesized by Dr. Manabe in Osaka University (6SLeC cluster [b], LeC cluster [c], and control clusters [d, e, f]). (B) Interaction between siglec-H and sugar chain clusters were analyzed by Biacore. Response increases when analyte and ligand interact. Siglec-H is immobilized on the sensor chip as a ligand. Analyte sugar chain clusters (0.5 μM each) were injected into Biacore. Response was observed when 6SLeC cluster (b) was injected. No signal was observed when control clusters (d, e, f) were injected. (C) Interaction between siglec-H and anti-siglec-H antibody was analyzed by Biacore. Siglec-H is immobilized on the sensor chip as a ligand. Response was observed when anti-siglec-H antibody (0.2 μM) was injected. No signal was observed when control rat IgG (0.2 μM) were injected. Signal of anti-siglec-H antibody was stronger than that of 6SLeC possibly because of the high MW of anti-siglec-H antibody. (D) Interaction between siglec-H and sugar chain clusters was analyzed by Biacore. Siglec-H is immobilized on the sensor chip as a ligand. Response was observed when 6SLeC cluster (b, 5.0 μM) was injected. No signal was observed when LeC cluster (c, 5.0 μM) were injected. The signal was observed

when the low-concentration of 6SLeC cluster (b, 1.0 μM) was injected. (E) Interaction between siglec-H and 6SLeC cluster were regulated in a dose-dependent manner (b, 1.0 to 8.0 μM).

Figure 9. Possible interaction between microglia and synapses obtained by my study and previous reports

Scheme for the predicted synthetic pathway of 6SLeC-containing sialylated A2G'2F, and interactions between sialylated A2G'2F and siglecs proposed in this study. Sialylation occurs in the Golgi apparatus. Sialic acids are transferred to terminal gal residues by ST3Gals. Furthermore, sialic acids are transferred to GalNAc residue through α2,6-linkage by ST6GalNAcs. ST6GalNAcV is a strong candidate for this reaction considering the its expression level in the brain and its substrate specificity. Sialylated A2G'2F is transported to the plasma membrane by A2G'2F-carrier proteins. There are various types of sialylated A2G'2F on the cell surface. Siglec-E binds to 6SLeC and α2,3-linked sialic acid. Siglec-E binds to disialyl-LeC weakly. Siglec-E inhibits microglial phagocytosis, thus showing neuroprotective effect. Apoptosis and malignant transformation induces desialylation of sialylated glycans by neuraminidases in the cytosol and plasma membrane. 6SLeC-containing sialylated-A2G'2F increases and by the desialylation of tri- and tetra-sialylated A2G'2F. Increased 6SLeC is recognized by siglec-H. Siglec-H induces the microglial phagocytosis of apoptotic neurons.

Table 1

Non-sialylated A2G’ 2F

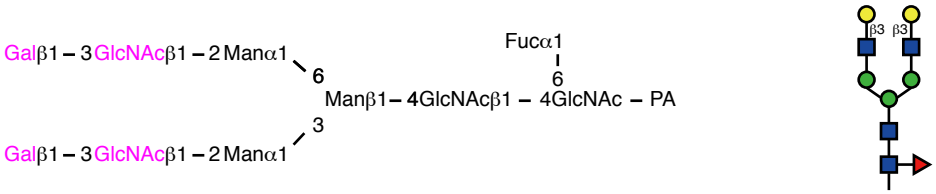

Mono-sialylated A2G’ 2F

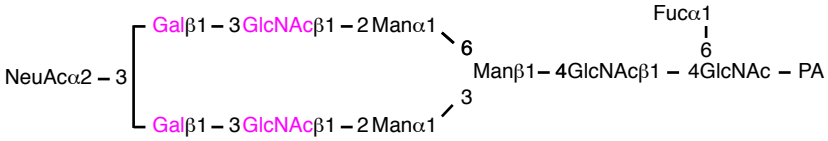

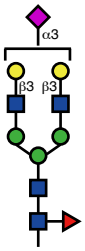

Di-sialylated A2G’ 2F

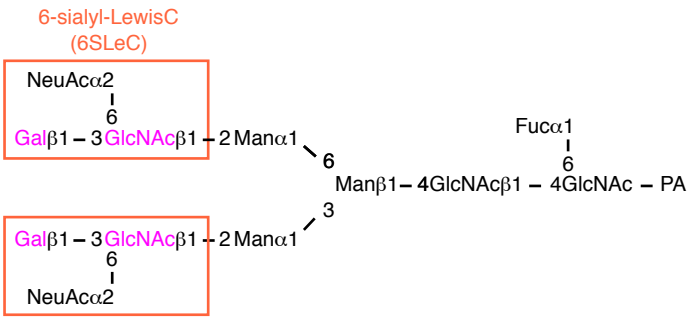

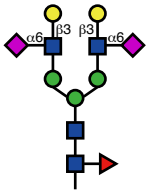

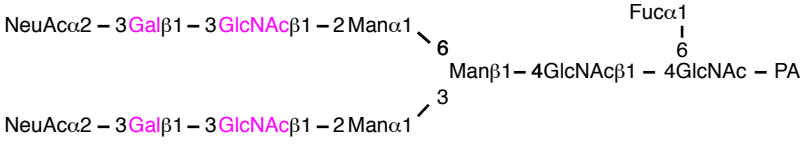

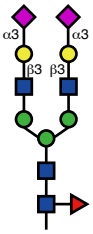

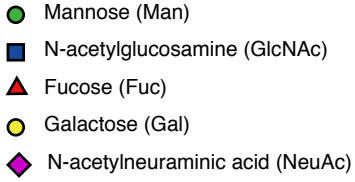

Table 1 continued

Tri-sialylated A2G’ 2F

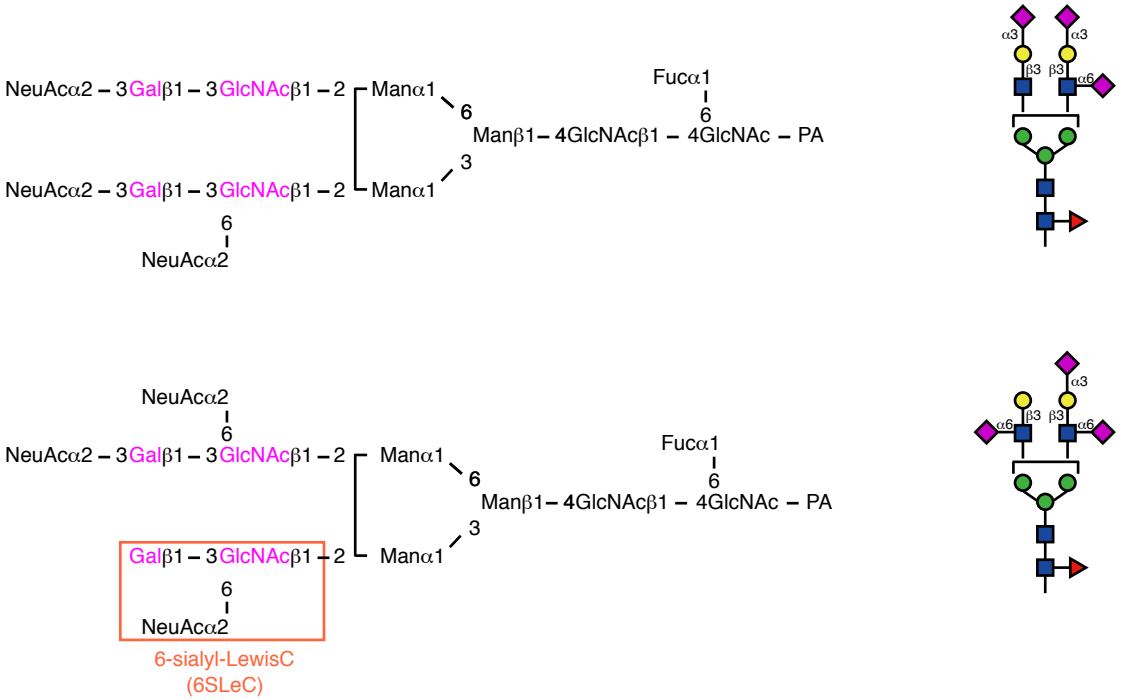

Tetra-sialylated A2G’ 2F

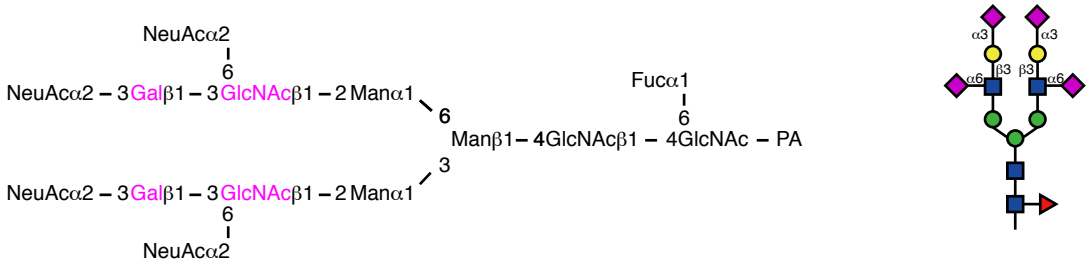

- Mannose (Man)
- N-acetylglucosamine (GlcNAc)
- Fucose (Fuc)
- Galactose (Gal)
- N-acetylneuraminic acid (NeuAc)

Determined structures of sialylated A2G’ 2F in the mouse brain.

Seven structures of sialylated A2G’ 2F were determined. Examples of Di- and Tri- sialylated A2G’ 2F harboring 6SLeC (orange box). More simplified figures of sialylated A2G’ 2F were drown on the right side.

Table 2

Detected protein	Score (Mascot)	Consensus (Asn-X-Ser/Thr)	Localization
NTM	336	7	Plasma membrane, Synapse
CRT	411	1	ER, Cytoplasm, Plasma membrane

Candidates for A2G' 2F-carrier proteins.

Many proteins were detected in gel pieces where A2G' 2F was detected. NTM and CRT were considered to be the carrier proteins because of the high score on Mascot software (more than 150), number of consensus sequence for N-glycosylation (more than 1), and localization in the cell (cell membrane).

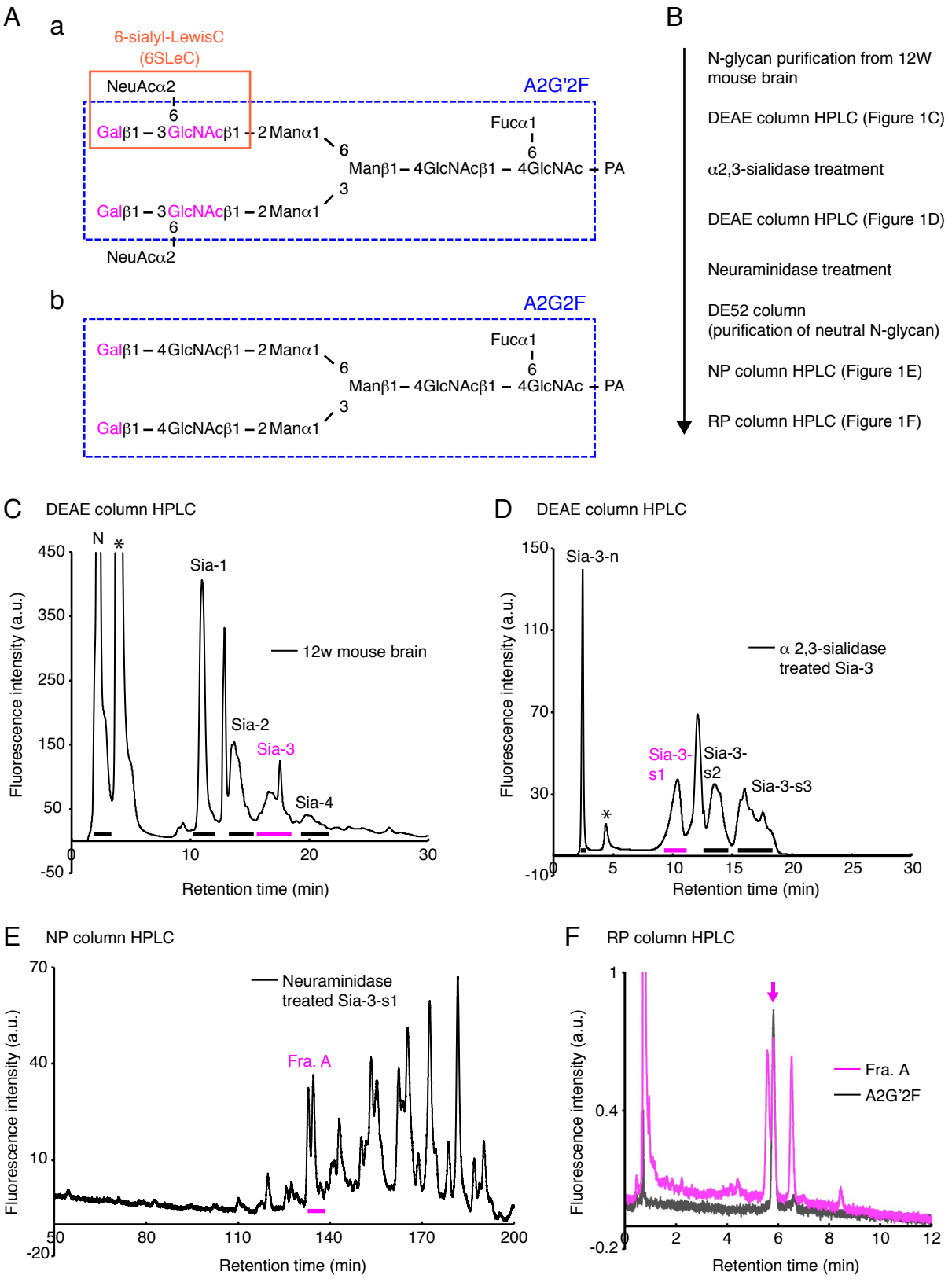
A
a
6-sialyl-LewisC
(6SLeC)
NeuAcα2
6
Galβ1 – 3GlcNAcβ1 – 2Manα1
6
Manβ1 – 4GlcNAcβ1 – 4GlcNAc – PA
3
Galβ1 – 3GlcNAcβ1 – 2Manα1
6
NeuAcα2
Fucα1
6
A2G'2F
b
Galβ1 – 4GlcNAcβ1 – 2Manα1
6
Manβ1 – 4GlcNAcβ1 – 4GlcNAc – PA
3
Galβ1 – 4GlcNAcβ1 – 2Manα1
Fucα1
6
A2G2F
B
N-glycan purification from 12W mouse brain
DEAE column HPLC (Figure 1C)
α2,3-sialidase treatment
DEAE column HPLC (Figure 1D)
Neuraminidase treatment
DE52 column
(purification of neutral N-glycan)
NP column HPLC (Figure 1E)
RP column HPLC (Figure 1F)
C
DEAE column HPLC
N
*
Sia-1
Sia-2
Sia-3
Sia-4
12w mouse brain
Fluorescence intensity (a.u.)
Retention time (min)
D
DEAE column HPLC
Sia-3-n
α 2,3-sialidase
treated Sia-3
Sia-3-s1
Sia-3-s2
Sia-3-s3
*
Fluorescence intensity (a.u.)
Retention time (min)
E
NP column HPLC
Neuraminidase
treated Sia-3-s1
Fra. A
Fluorescence intensity (a.u.)
Retention time (min)
F
RP column HPLC
Fra. A
A2G'2F
Fluorescence intensity (a.u.)
Retention time (min)

Figure 1

A

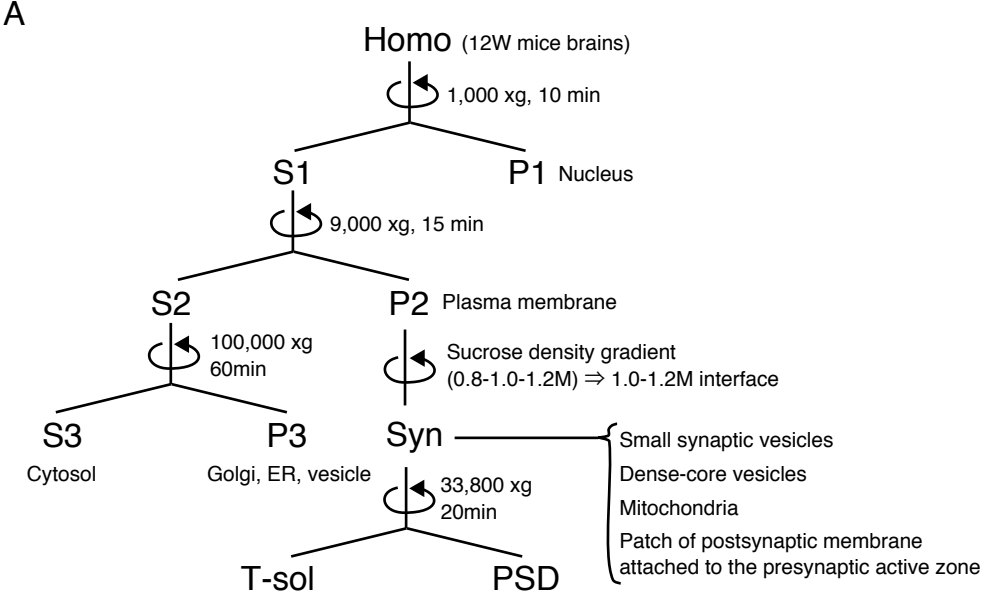
Homo (12W mice brains)
1,000 xg, 10 min
S1
P1 Nucleus
9,000 xg, 15 min
S2
P2 Plasma membrane
100,000 xg
60min
Sucrose density gradient
(0.8-1.0-1.2M) ⇒ 1.0-1.2M interface
S3
Cytosol
P3
Golgi, ER, vesicle
Syn
33,800 xg
20min
T-sol
PSD
Small synaptic vesicles
Dense-core vesicles
Mitochondria
Patch of postsynaptic membrane
attached to the presynaptic active zone

B

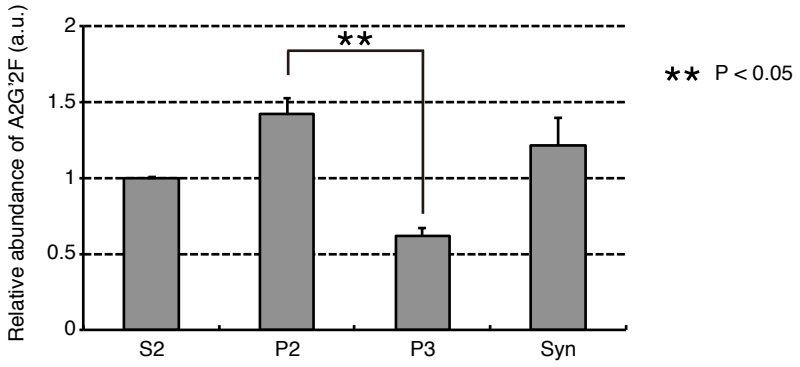
Relative abundance of A2G'2F (a.u.)
2
1.5
1
0.5
0
**
S2
P2
P3
Syn
** P < 0.05

Figure 2

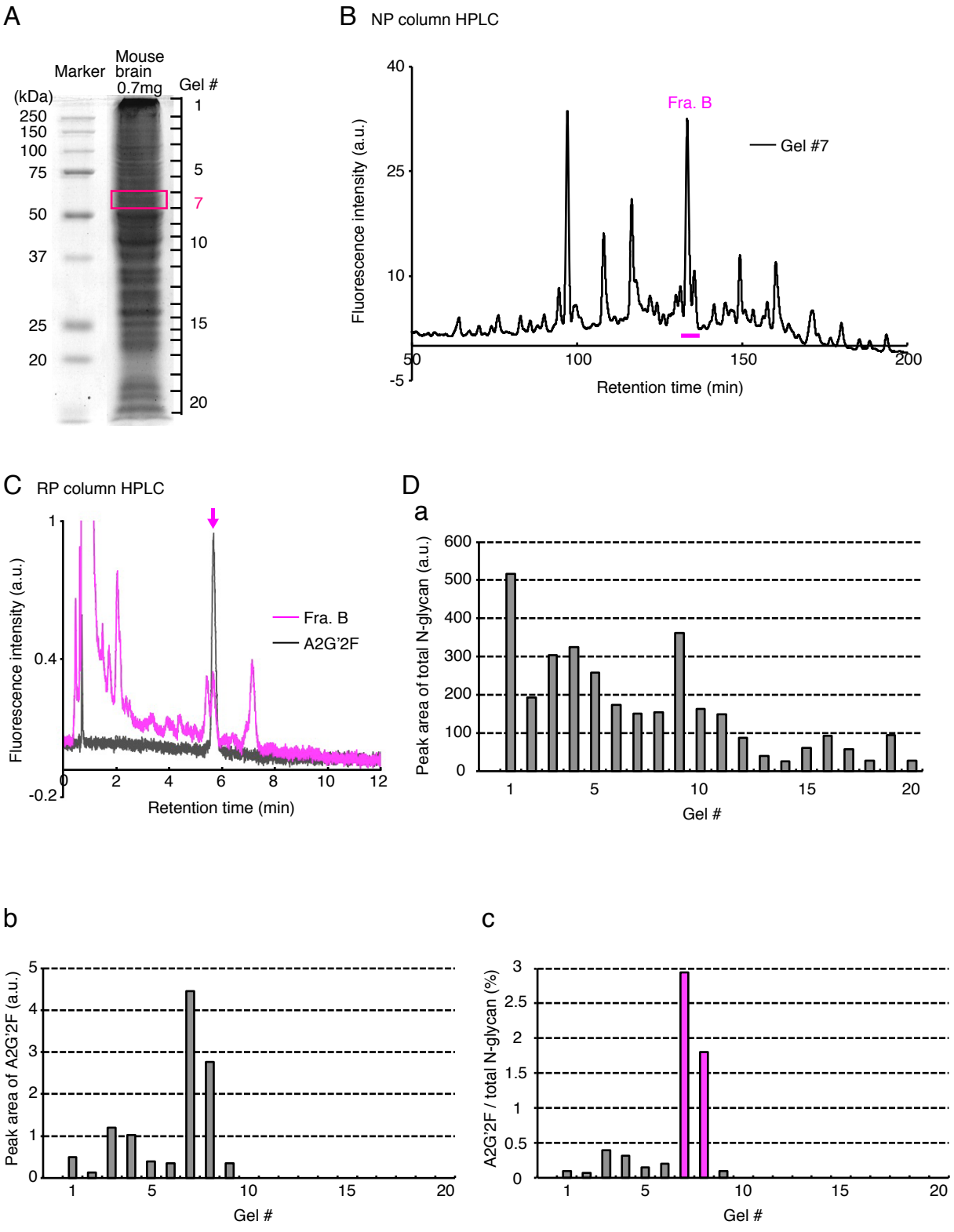
A
Marker
Mouse brain 0.7mg
Gel #
(kDa)
250
150
100
75
50
37
25
20
1
5
7
10
15
20
B NP column HPLC
Fra. B
Gel #7
Fluorescence intensity (a.u.)
Retention time (min)
C RP column HPLC
Fra. B
A2G'2F
Fluorescence intensity (a.u.)
Retention time (min)
D
a
Peak area of total N-glycan (a.u.)
Gel #
b
Peak area of A2G'2F (a.u.)
Gel #
c
A2G'2F / total N-glycan (%)
Gel #

Figure 3

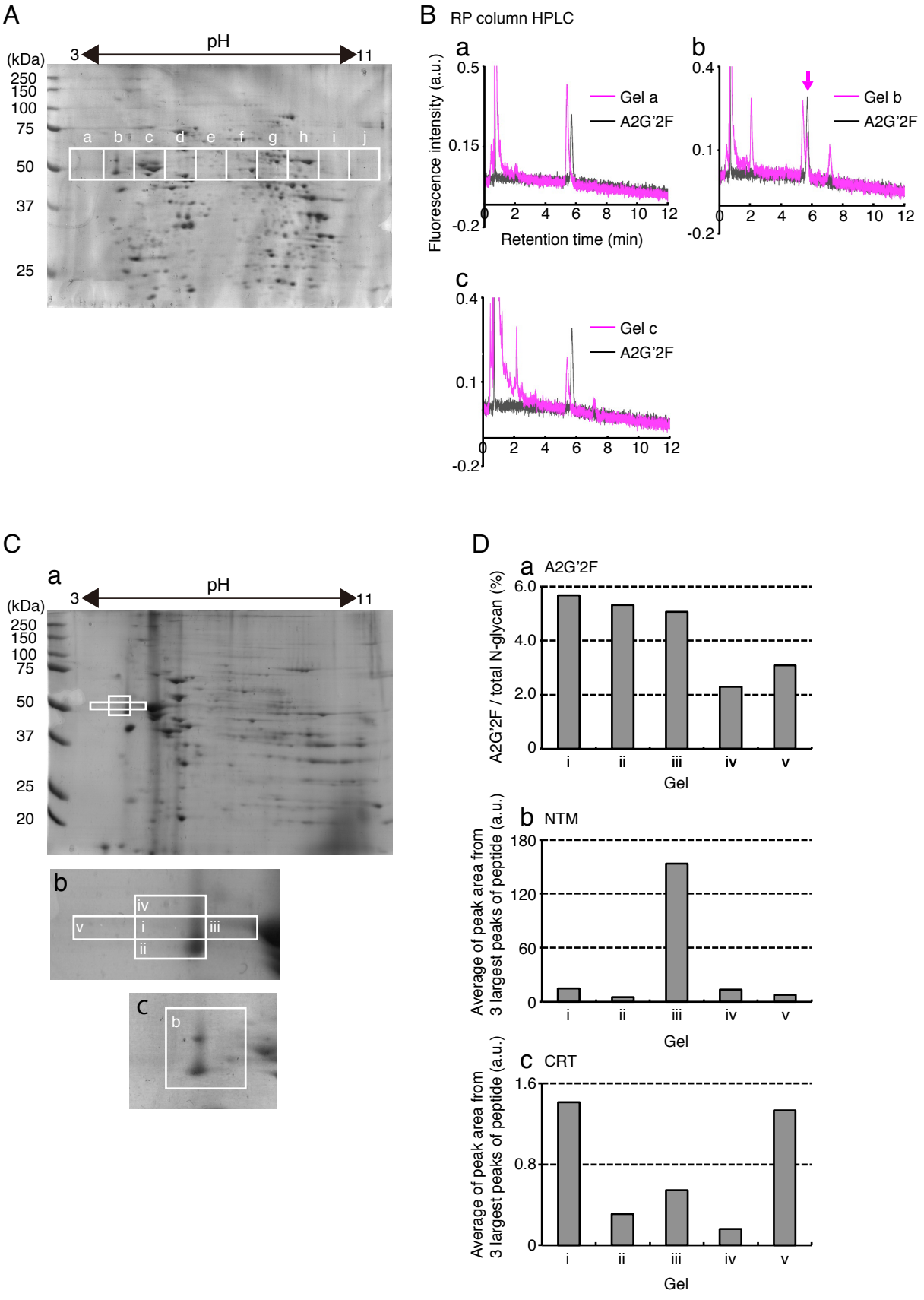
A
pH
3
11
(kDa)
250
150
100
75
50
37
25
a b c d e f g h i j
B RP column HPLC
a
b
c
Gel a
Gel b
Gel c
A2G'2F
Fluorescence intensity (a.u.)
Retention time (min)
C
a
b
c
iv
v
i
iii
ii
20
D
a A2G'2F
A2G'2F / total N-glycan (%)
b NTM
Average of peak area from 3 largest peaks of peptide (a.u.)
c CRT
Gel

Figure 4

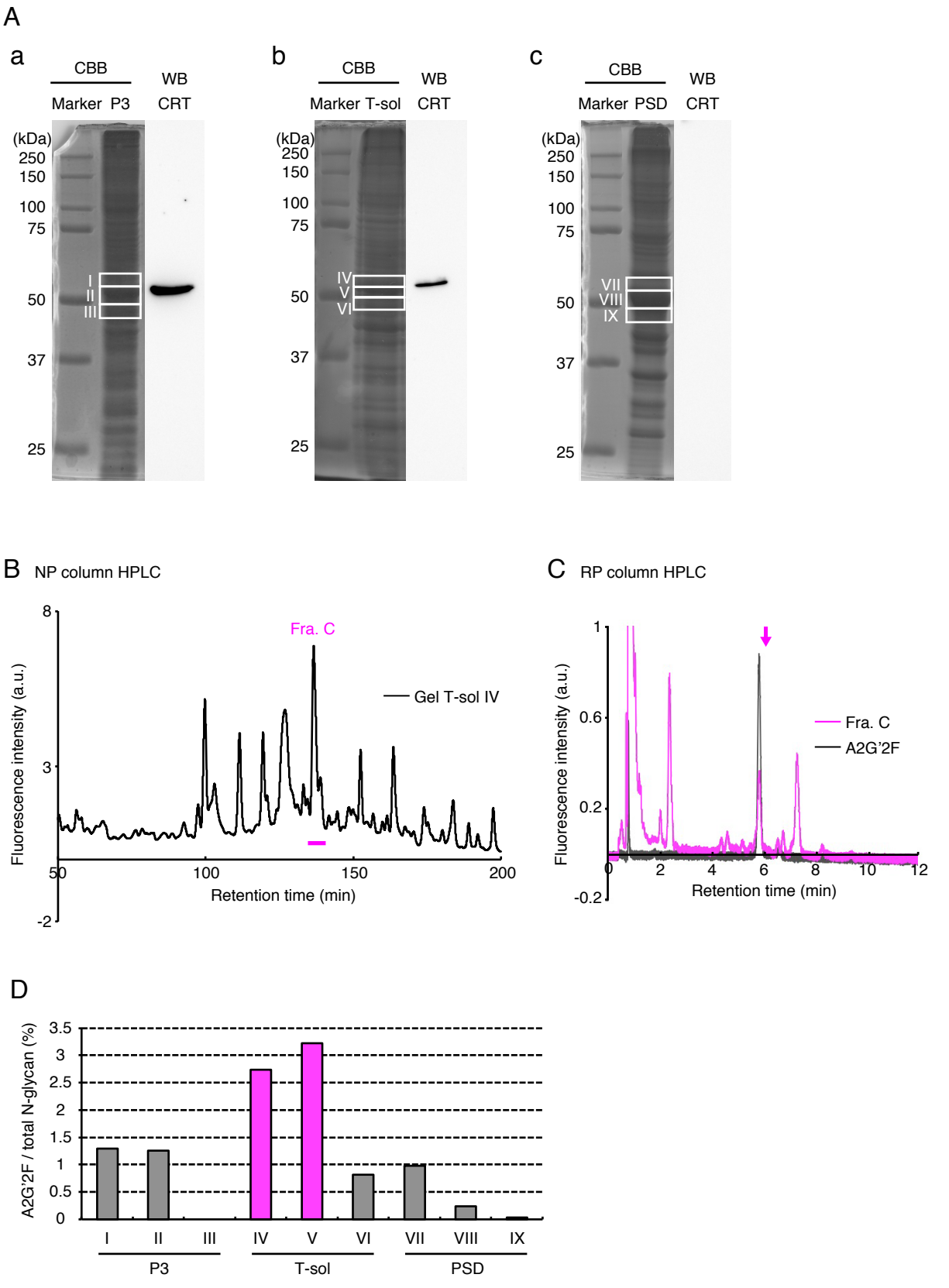
A
a
CBB
WB
Marker P3
CRT
(kDa)
250
150
100
75
50
37
25
I
II
III
b
Marker T-sol
IV
V
VI
c
Marker PSD
VII
VIII
IX
B NP column HPLC
Fra. C
Gel T-sol IV
Fluorescence intensity (a.u.)
Retention time (min)
C RP column HPLC
Fra. C
A2G'2F
D
A2G'2F / total N-glycan (%)
P3
T-sol
PSD

Figure 5

A

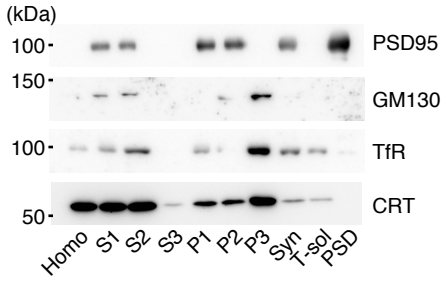
(kDa)
100
150
100
50
PSD95
GM130
TfR
CRT
Homo
S1
S2
S3
P1
P2
P3
Syn
T-sol
PSD

B

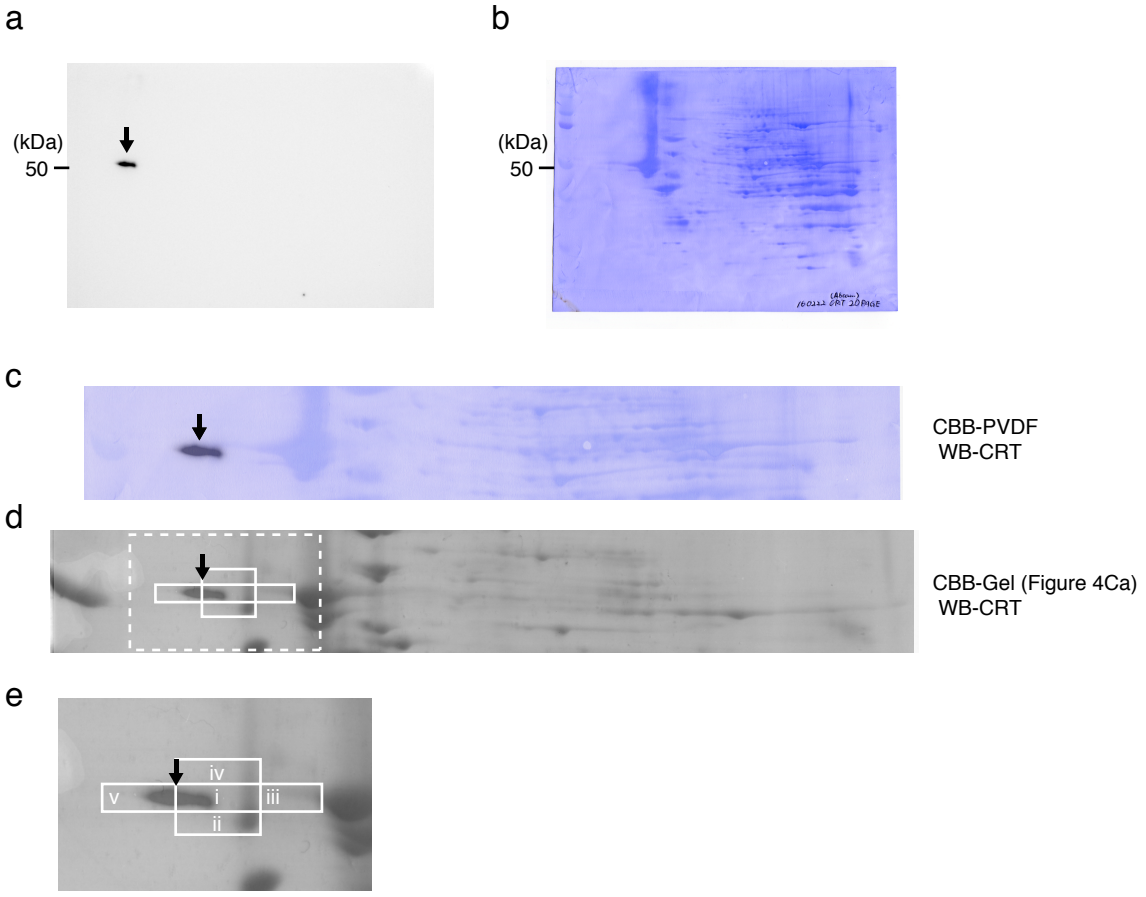
a
b
(kDa)
50
(kDa)
50
c
CBB-PVDF
WB-CRT
d
CBB-Gel (Figure 4Ca)
WB-CRT
e
iv
v
i
iii
ii

Figure 6

A

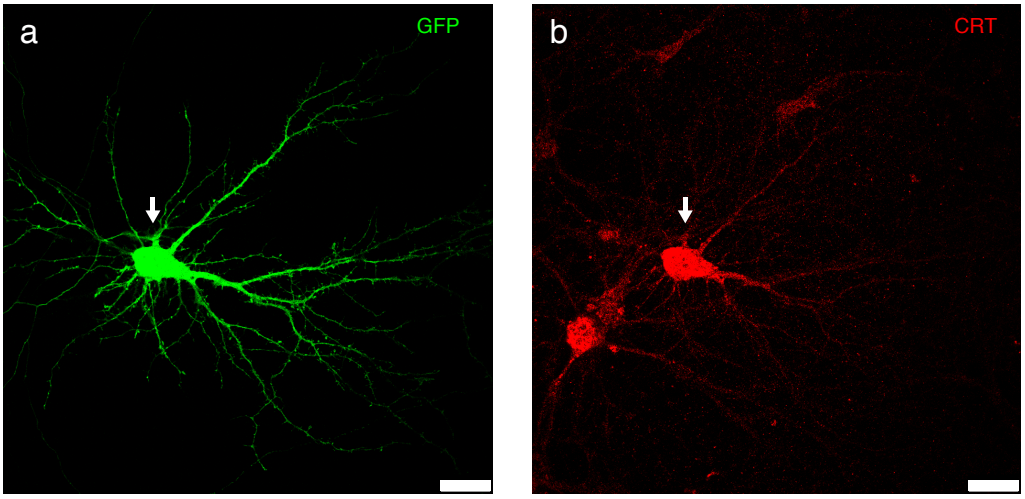
a
GFP
b
CRT

B

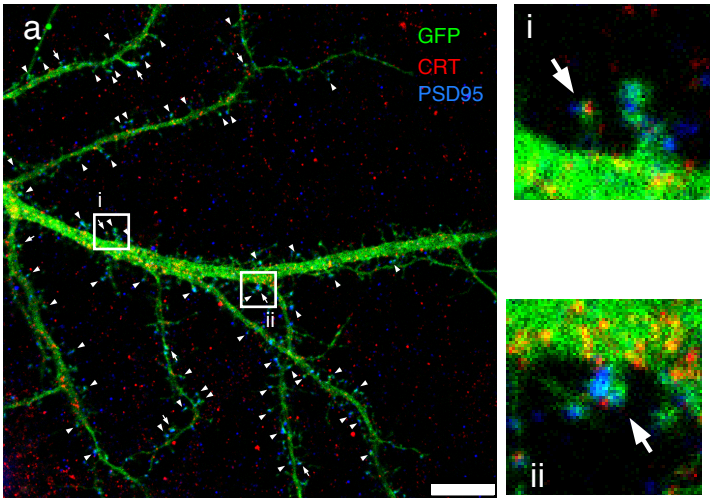
a
GFP
CRT
PSD95
i
ii
i
ii

C

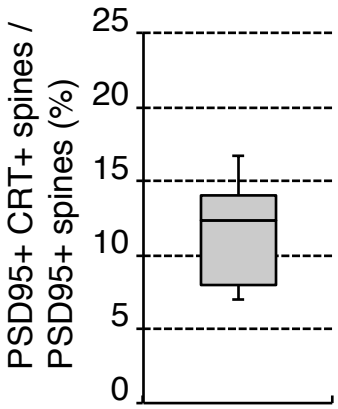
PSD95+ CRT+ spines /
PSD95+ spines (%)
25
20
15
10
5
0

Figure 7

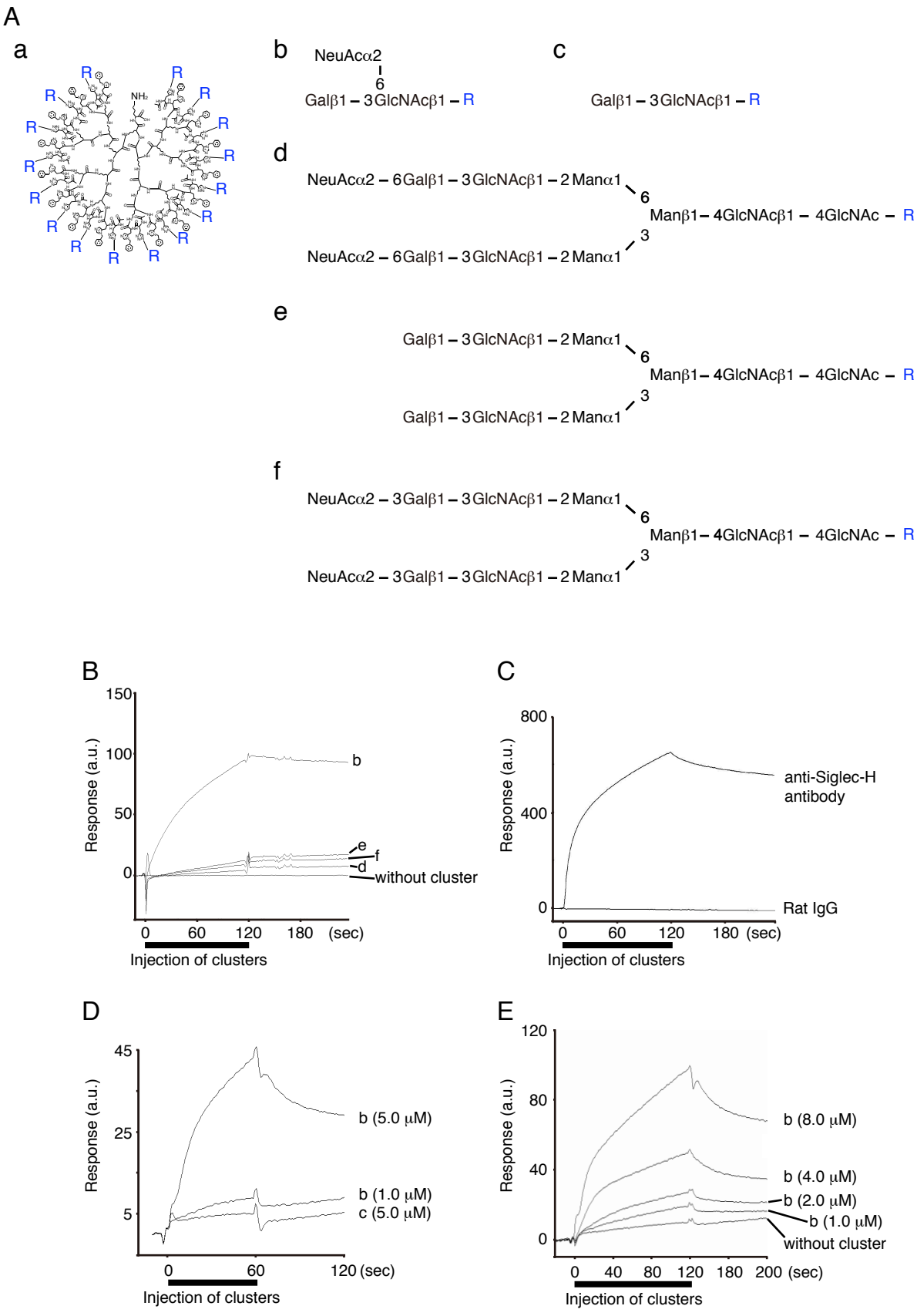
A
a
b
NeuAcα2
6
Galβ1 – 3GlcNAcβ1 – R
c
Galβ1 – 3GlcNAcβ1 – R
d
NeuAcα2 – 6Galβ1 – 3GlcNAcβ1 – 2Manα1
6
Manβ1– 4GlcNAcβ1 – 4GlcNAc – R
3
NeuAcα2 – 6Galβ1 – 3GlcNAcβ1 – 2Manα1
e
Galβ1 – 3GlcNAcβ1 – 2Manα1
6
Manβ1– 4GlcNAcβ1 – 4GlcNAc – R
3
Galβ1 – 3GlcNAcβ1 – 2Manα1
f
NeuAcα2 – 3Galβ1 – 3GlcNAcβ1 – 2Manα1
6
Manβ1– 4GlcNAcβ1 – 4GlcNAc – R
3
NeuAcα2 – 3Galβ1 – 3GlcNAcβ1 – 2Manα1
B
Response (a.u.)
150
100
50
0
b
e
f
d
without cluster
0 60 120 180 (sec)
Injection of clusters
C
Response (a.u.)
800
400
0
anti-Siglec-H antibody
Rat IgG
0 60 120 180 (sec)
Injection of clusters
D
Response (a.u.)
45
25
5
b (5.0 μM)
b (1.0 μM)
c (5.0 μM)
0 60 120 (sec)
Injection of clusters
E
Response (a.u.)
120
80
40
0
b (8.0 μM)
b (4.0 μM)
b (2.0 μM)
b (1.0 μM)
without cluster
0 40 80 120 180 200 (sec)
Injection of clusters

Figure 8

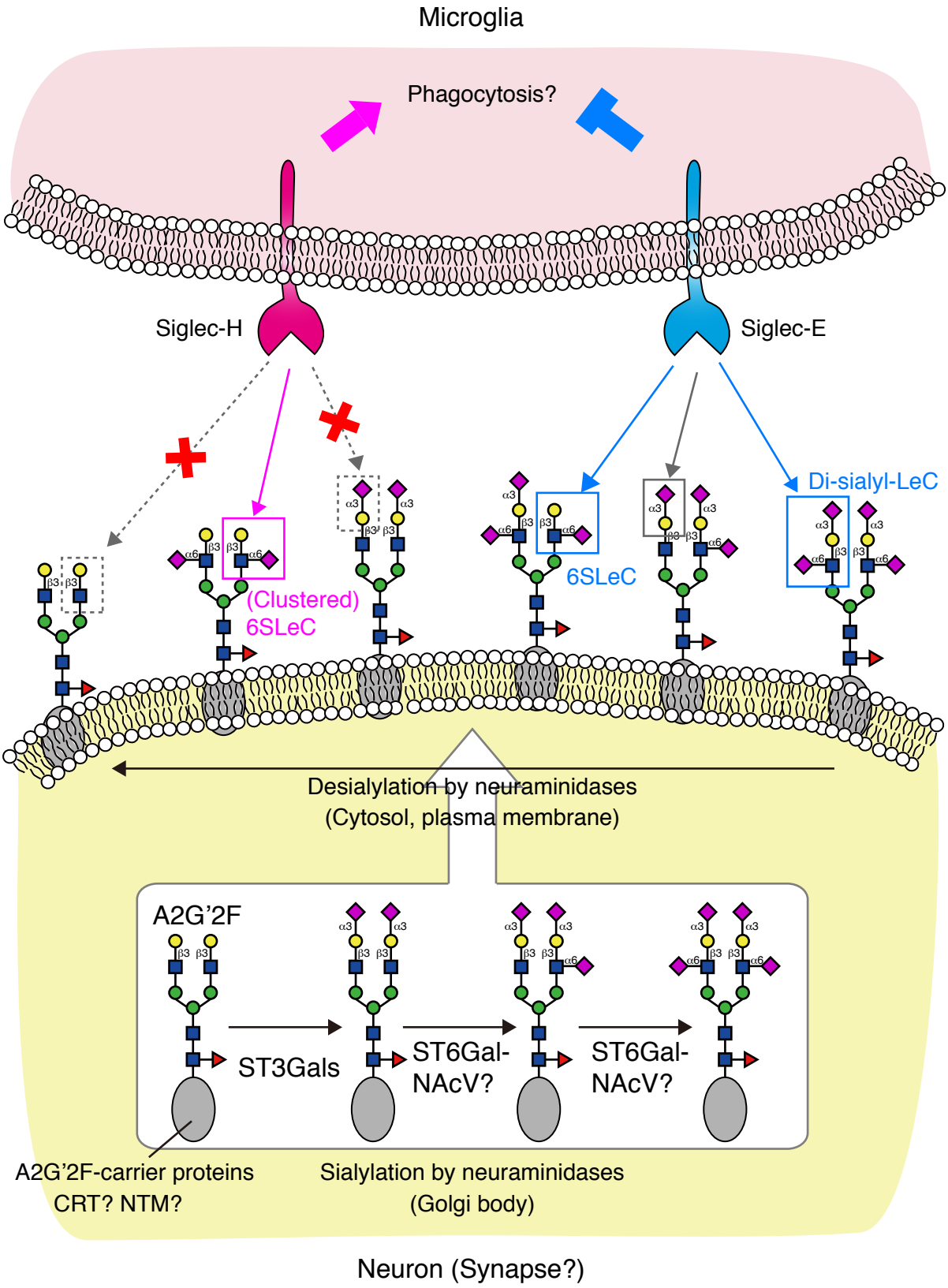
Microglia
Phagocytosis?
Siglec-H
Siglec-E
(Clustered)
6SLeC
6SLeC
Di-sialyl-LeC
Desialylation by neuraminidases
(Cytosol, plasma membrane)
A2G'2F
ST3Gals
ST6Gal-
NAcV?
ST6Gal-
NAcV?
A2G'2F-carrier proteins
CRT? NTM?
Sialylation by neuraminidases
(Golgi body)
Neuron (Synapse?)

Figure 9